AD NUMBER

AD873037

LIMITATION CHANGES

TO:

Approved for public release; distribution is unlimited.

FROM:

**Distribution authorized to U.S. Gov't. agencies and their contractors;
Administrative/Operational Use; MAY 1970. Other requests shall be referred to Army Aviation Materiel Labs., Fort Eustis, VA 23604.**

AUTHORITY

USAAVLABS ltr 18 Jan 1971

USAAVLABS TECHNICAL REPORT 70-26

APPLICATION OF THE NORTHROP ROTATIONAL SIMULATOR TO HELICOPTERS AND V/STOL AIRCRAFT (USER'S GUIDE)

By

John B. Sinacori

May 1970

U. S. ARMY AVIATION MATERIEL LABORATORIES
FORT EUSTIS, VIRGINIA

CONTRACT DAAJ02-68-C-0019
NORTHROP CORPORATION
AIRCRAFT DIVISION
HAWTHORNE, CALIFORNIA

DISCLAIMERS

The findings in this report are not to be construed as an official Department of the Army position unless so designated by other authorized documents.

When Government drawings, specifications, or other data are used for any purpose other than in connection with a definitely related Government procurement operation, the United States Government thereby incurs no responsibility nor any obligation whatsoever; and the fact that the Government may have formulated, furnished, or in any way supplied the said drawings, specifications, or other data is not to be regarded by implication or otherwise as in any manner licensing the holder or any other person or corporation, or conveying any rights or permission, to manufacture, use, or sell any patented invention that may in any way be related thereto.

Trade names cited in this report do not constitute an official endorsement or approval of the use of such commercial hardware or software.

DISPOSITION INSTRUCTIONS

Destroy this report when no longer needed Do not return it to the originator.

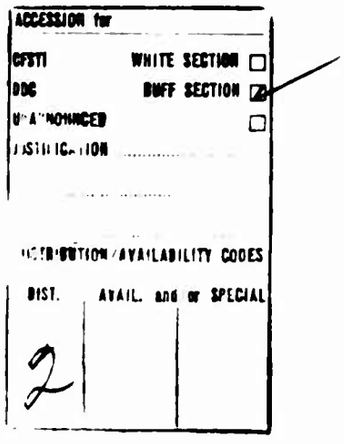

DEPARTMENT OF THE ARMY
HEADQUARTERS US ARMY AVIATION MATERIEL LABORATORIES
FORT EUSTIS, VIRGINIA 23604

This report has been reviewed by the U. S. Army Aviation Materiel Laboratories and is considered to be technically sound. The work was performed under Contract DAAJ02-68-C-0019. The report is published for the dissemination and application of information and the stimulation of ideas in the area of simulation technology, with emphasis on handling qualities research.

Task 1F162204A14233
Contract DAAJ02-68-C-0019
USAAVLABS Technical Report 70-26
May 1970

APPLICATION OF THE NORTHROP ROTATIONAL SIMULATOR TO HELICOPTERS AND V/STOL AIRCRAFT (USER'S GUIDE)

NOR-70-6

By

J.B. Sinacori

Prepared by

Northrop Corporation
Aircraft Division
Hawthorne, California

for

U.S. ARMY AVIATION MATERIEL LABORATORIES

FORT EUSTIS, VIRGINIA

SUMMARY

The Northrop Aircraft rotational three-axis flight simulator was developed to simulate flight tasks requiring visual stimuli of the outside real-world environment for the pilot. Takeoff and landing, and general low-altitude operations are examples. The purpose of this document is to suggest guidelines to be used in developing software interface computations to effectively integrate the pilot and mathematical vehicular representation to the Northrop simulator.

The visual and cockpit motion performance is designed to meet some of the more important physiological requirements related to the flight envelope of all V/STOL and conventional aircraft. The external world display is produced by the DeFlorez point light source technique. A high-intensity point light source projects shadows of scale models of real-world objects onto a spherical reflecting screen. The image is projected in color with terrain texture and three-dimensional representation of display objects with appropriate perspective size and position. Some validation methods are described with suggestions for their use based on the type of simulation desired. These include pilot opinion rating, numerical and statistical analysis methods, and combinations of both depending on the degree of validation required.

Suggested interface mechanizations are given which provide accurate visual reference stimuli without appreciable distortion. The sensation of lateral and longitudinal acceleration is produced by tilting with respect to the gravitational vector due to the lack of large linear motions.

A rationale is included which assists the user to assess the probability of success for any particular type of simulation. This document is intended to assist in the preparation of an experimental design and development of the interface computations. It is considered by no means complete, and it is hoped that revisions and additions are forthcoming from subsequent users.

FOREWORD

This final technical report covers part of the work performed by Northrop Corporation, Aircraft Division during the period 1 February 1968 to 1 January 1970. It was sponsored by the U. S. Army Aviation Materiel Laboratories, Ft. Eustis, Virginia, and was monitored by Mr. Robert P. Smith of the Aeromechanics Division. The work was authorized by DA Task 1F162204A14233.

The program at Northrop was performed by the Research and Technology Department, with Mr. J.B. Sinacori serving as Principal Investigator. Northrop Report number 70-6 has been assigned for internal control.

The author wishes to thank the many people who contributed generously to the effort, particularly Messrs. H.D. Cooles, D.M. Patton, W.I. Greenwood, and G.R. Mills of the Northrop Aerosciences Laboratory. Special thanks are due to Mr. N. Albion of Boeing-Vertol for his excellent criticisms.

BLANK PAGE

CONTENTS

LIST OF ILLUSTRATIONS

LIST OF TABLES

LIST OF SYMBOLS

db	decibels
F	force, lbs
g	acceleration of gravity, ft/sec^2
g_x	gravitational acceleration along the x body axis, ft/sec^2
g_y	gravitational acceleration along the y body axis, ft/sec^2
g_z	gravitational acceleration along the z body axis, ft/sec^2
G	simulator actuator position, ft or in.
$G(\omega)$	amplitude ratio
H	vertical displacement from the point light source, positive down, in.
Hz or HZ	frequency, cycles/sec
K	gain
K_p	position gain, volts/rad
K_v	velocity gain, volts/rad/sec
m	vehicle mass, slugs
p,q,r	vehicle rates about the body axes x, y, and z respectively, rad/sec or deg/sec
R	screen radius, ft
S	visual display transparency scale; ratio of real-world dimension to model dimension
s	Laplace transform variable
u,v,w	vehicle velocities along the x,y, and z body axes respectively, ft/sec

$\dot{U}_{OBS}$	longitudinal (x body axis) observed acceleration, ft/sec^2
$\dot{V}_{OBS}$	lateral (y body axis) observed acceleration, ft/sec^2
$\dot{V}$	inertial acceleration, ft/sec^2
$\dot{W}_{OBS}$	normal (z body axis) observed acceleration, ft/sec^2
X	north-south earth coordinate; positive north, ft; or translational actuator position, ft
Y	east-west earth coordinate, positive east, ft; or translational actuator position, ft
Z	vertical earth coordinate, positive down, ft; or translational actuator position, ft
x	longitudinal displacement along the x body axis, ft
y	lateral displacement along the y body axis, ft
z	normal displacement along the z body axis, ft
δ_1	true depression angle of ground object, rad or deg
δ_2	displayed depression angle of ground object, rad or deg
μ_f	microfarad
τ	filter time constant, sec
φ	bank angle, deg or rad
θ	pitch angle, deg or rad
Ψ	heading angle, deg or rad
ω	frequency, cycles/sec

Subscripts or Sub-Subscripts

D	visual display subsystem
F	feedback
M	motion subsystem
p,q,r	angular rates about the x,y, and z body axes respectively

P_e	pilot's eye center; a point midway between the eyes
X	simulator longitudinal axis
Y	simulator lateral axis
Z	simulator normal axis
Ψ	simulator roll angle
θ	simulator pitch angle
Ψ	simulator yaw angle
1	yaw→pitch→roll Euler angle transforms
2	yaw→roll→pitch Euler angle transforms

NOTE:

1)	A dot over a quantity indicates differentiation with respect to time
2)	$\wedge$ over a quantity indicates total command voltage
3)	$\measuredangle$ denotes phase angle
4)	$\|\|$ denotes absolute value
5)	Σ denotes summation

INTRODUCTION

The intent of the report is to provide the simulator user with information which can be used to guide the development of the software interface computations required to effectively integrate the pilot with the mathematical representation of the vehicle. It is assumed that a valid mathematical representation is available and that the equations can be solved in real time.

This report attempts to do the following:

1. Detail the quantities required from the vehicle equations of motion for the drive mechanizations and describe in detail two drive mechanizations.

2. Provide the rationale for the selection of required simulator equipment.

3. Describe checkout and performance measurement techniques.

4. Suggest validation techniques.

5 Outline operating procedures.

In addition, certain precautionary procedures are described which hopefully will increase operating efficiency and enable the user to interpret malfunctions. It is stressed here that a good working knowledge of the flight characteristics of the vehicle is extremely helpful but not necessary since the user will certainly acquire this knowledge as the simulation progresses.

SIMULATOR CHARACTERISTICS

GENERAL DESCRIPTION

The Northrop rotational flight simulator is a device which includes a cockpit shell mounted on a motion base. The motion base assembly is floor-mounted near the center of a room which contains a spherical reflecting screen. Near the center of this screen and above the cockpit, a transparent plate is carried by a series of six gimbals, the outer one of which is fastened to a s ructure supported by four floor-mounted massive columns.

At the center of the screen and above the transparent plate, an intense point light source is room-mounted. Eleven hydraulic actuators are used to drive the transparent plate and motion system. A control console is provided which mounts the hydraulic and electrical control and monitoring equipment. A general arrangement of the rotational flight simulator is shown in Figure 1.

Visual Display Principle

The visual display is of the DeFlorez type. A transparent plate carries transparent scale models of real-world objects such as hangars, runways, aircraft, etc. A point light source is rigidly mounted to the room just above the plate. A spherical reflecting screen, with center at the light source, wraps 200° around the plate and mounting gimbal assembly. The perspective view of the plate as seen at the point light source is projected via shadows onto the screen. If an observer views the screen from a point just below the plate and close to the point light source, the images observed will closely resemble but not exactly match the view as seen from the point light source. This is so for two reasons. First, the projected scene is composed of the shadows of the objects, and second, the scene is distorted depending on the geometrical relation between the observer and the point light source in comparison to the screen radius. This is illustrated by Figure 2, in which a typical depression angle for a ground object is represented by the visual display. For the case where the observer's eye point is directly beneath the light,

$$\tan \delta_2 = \tan \delta_1 - (H_{p_e}/R)\sec \delta_1 \qquad (1)$$

The relation shows that the error is a maximum at $\delta_1 = 0$ and zero at $\delta_1 = \pi/2$.

The maximum angular error is of course equal to - $\sin^{-1}(H_{p_e}/R)$. The negative sign reveals that the projected horizon is above the actual horizon. This is in effect a statement of the "bowl" effect or the fact that the projected world appears to resemble a bowl with the observer near the center.

Of possible greater importance, physiologically speaking, is the appearance of the projected scene under dynamic conditions. This will be discussed after the next paragraph on the dynamic aspects of the optical system.

Since the view of the model world as seen from the point light source is approximately projected on the spherical screen when viewed from a point near its center, the illusion of movement may be easily created by moving the transparent plate with respect to the light. This is accomplished by a series of six hydraulically actuated gimbals which impart to the plate three orthogonal rotations and three orthogonal translations. The gimbal and actuator arrangements are shown in Figure 3.

Because the distortions as described above exist under static conditions, they also exist under dynamic conditions. Dynamic distortions are observed as "stretching" of the projected world depending on where in the visual field the projection is placed and where the observer's eye is located with respect to the point light source. The projected world therefore will not remain rigid-appearing when either rotational or translatory motions are imparted to the plate. This apparent "flexibility" affects pilot performance in the simulator during certain tasks and is probably one of the causes of initial, but brief, nausea onset when an experienced pilot enters the simulator for the first time.

Since it is not possible at this time to relate physiological requirements to display imperfections, no further discussion of these imperfections will be related here. If the user is interested in the geometrical imperfections of the DeFlorez system, Reference 1 will provide more information on this subject.

At the time of writing, four transparencies are available. Three are scale models of the Mustang stagefield area at Ft. Wolters, Texas at scales of 100, 550, and 2000 to one.* The remaining plate is a commercially manufactured one of an airport at a scale of 750 to one. The measured available dimensions for maneuvering for each plate are listed in Table I.

---

*Transparency scale is defined as the ratio of any real world dimension to the corresponding model dimension and will be denoted by S.

TABLE I. VISUAL DISPLAY MANEUVERING RANGE (FEET)				
Direction	Plate Scale			
	S = 100	S = 550	S = 750	S = 2000
X	± 200	± 1100	± 1500	± 4000
Y	± 200	± 1100	± 1500	± 4000
Z	83	458	625	1666

Motion Base

A five-degree-of-freedom motion base is provided which can be used in a variety of ways. Input wiring to five hydraulic actuators is implemented in the control console and is arranged so that only single input voltages are required to achieve cockpit pitch, roll, and yaw motions and longitudinal and vertical translations. The actuators and gimbals are actually arranged as follows: two vertical, two longitudinal, and one isolated for pitch. Collective use of the vertical actuators results in vertical (or heave) motions. Differential use of the vertical actuators results in roll. The same argument applies to the horizontal pair of actuators for longitudinal movement and yaw respectively. The motion base gimbal and actuator arrangement is shown in Figure 4.

A single-place cockpit is arranged so that modifications can be made quickly and easily. Unfortunately, no overhead controls or cockpit panels may be used because they will interfere with the visual display. The cockpit is single place because of early design. This is a happy outcome, however, since in its present configuration, visual display distortions described in a later section are minimized. A photo of the installation for the OH-13G helicopter is shown in Figure 5.

GENERAL PERFORMANCE

Coordinate System

The coordinate system used to describe the movements of the visual display is an orthogonal right-hand axis system fixed to the room with origin 5 inches below the point light source. Orientation of the plate in attitude is expressed by Euler angles referenced to the axis system just described. The order of rotation of these angles is pitch → roll → yaw starting from the room structure. The order, therefore, in expressing the orientation with respect to the plate (or Earth) is the reverse, or yaw → roll → pitch.

The same discussion applies to the cockpit motion base except that the origin is 4 feet below the point light source. The gimbal order is (not by design) the same as that for the visual display. This results in a fortunate situation when describing the first-order equations for the projected orientation in the presence of cockpit motion. This will be discussed further in the Mechanization section. Both coordinate systems with their related nomenclatures are shown in Figure 6.

Static Data

Calibration, Maximum Travels and Limit Switches

Figures 7 through 17 contain the static input and feedback voltage calibrations for all the hydraulic actuators for the visual display and motion subsystems. They are presented to give the user computer output and feedback scaling required and also to illustrate the linearity. Measurement accuracy for these data is about ±0.05 volt, ±0.002 foot and ±0.03 degree. Nominal limit switch positions are shown in each graph. Selection of computer limits below the limit switch voltage value may not always prevent resetting because of the actuator's step response. A high impedance input is necessary for the active feedback voltages in order to avoid "loading down" the feedback power supplies and thereby changing the input calibration. All actuators on the motion system have an independent or passive feedback system. Loading down of these systems will not affect the input calibration but will require a calibration check.

Thresholds

Thresholds are defined as the minimum step input voltage change required to obtain a measureable change in actuator position as indicated by the position feedback element. Their existence is caused by many factors, some of them highly variable with time. Among these are valve friction, cylinder and load friction, cylinder stiffness, load position, and feedback resolution. Some measurements have been made for the visual display actuators, and the results are shown in Table II. Also tabulated

are the corresponding position thresholds for each of the available transparencies.

TABLE II. VISUAL DISPLAY TRANSLATIONAL THRESHOLDS (FEET)

Actuator	Plate Scale S=1 (Basic)	S=100	S=550	S=750	S=2000
G_{X_D}	0.006	0.6	3.3	4.5	12
G_{Y_D}	0.004	0.4	2.2	3.0	8
G_{Z_D}	0.005	0.5	2.75	3.75	10

The rotational actuators' thresholds are, of course, independent of transparency scale and are listed in Table III.

TABLE III. VISUAL DISPLAY ROTATIONAL THRESHOLDS

ACTUATOR	THRESHOLDS
G_{φ_D}	0.026°
G_{θ_D}	0.017°
$\dot{G}_{\Psi_D}$	0.7°/Sec

Dynamic Data

Power Performance

Figure 18 contains the logarithmic power performance for the visual display roll actuator, G_{φ_D}. It is based upon the maximum displacement limit of ±0.35 radian, a maximum velocity limit of 0.7 rad/sec, and a maximum acceleration limit of 4 rad/sec^2. The plot is obtained from the relations which exist among peak displacement, velocity and acceleration during sinusoidal motion. The gray area included by the boundaries represents the available performance envelopes for the actuator. The minimum threshold is also shown. However, it is based on step response data.

Performance plots for the remaining ten actuators may be constructed using Figure 18 and the following limit data for all actuators shown in Tables IV and V.

TABLE IV. PERFORMANCE LIMITATIONS FOR THE VISUAL DISPLAY ACTUATORS

Actuator	Displacement (rad)	Displacement (deg)	Velocity (rad/sec)	Velocity (deg/sec)	Acceleration (rad/sec^2)	Acceleration (deg/sec^2)
G_{θ_D}	+0.350 -0.323	+20 -18.5	±0.7	±40.1	±4	±229
G_{φ_D}	+0.307 -0.328	+17.6 -18.8	±0.7	±40.1	±4	±229
G_{ψ_D}	Continuous		±1	±57.3	±1.5	±86
G_{X_D}	+1.93 ft -1.88 ft		±1 ft/sec		±0.09 ft/sec^2	
G_{Y_D}	+1.95 ft -1.92 ft		±1 ft/sec		±0.09 ft/sec^2	
G_{Z_D}	+0.350 ft -0.306 ft		±0.2 ft/sec		±0.09 ft/sec^2	

TABLE V. PERFORMANCE LIMITATIONS FOR THE MOTION BASE

Actuator	Displacement (rad)	Displacement (deg)	Velocity (rad/sec)	Velocity (deg/sec)	Acceleration (rad/sec^2)	Acceleration (deg/sec^2)
G_{θ_M}	+0.168 -0.180	+9.6 -10.3	±1.1	±63	±0.236	±13.5
G_{φ_M}	+0.241 -0.209	+13.8 -12.0	±0.523	±30	±1.4	±80.2
G_{ψ_M}	+0.145 -0.127	+8.3 -7.3	±0.523	±30	±1.4	±80.2
G_{X_M}	+0.309 ft -0.283 ft		±1.08 ft/sec		±22.5 ft/sec^2	
G_{Z_M}	+0.51 ft -0.47 ft		±1.08 ft/sec		±22.5 ft/sec^2	

Frequency Response Data and Required Compensation

Figures 19 through 24 show measured frequency response data for all actuators in the visual display and motion system. Measurement accuracy is about ± 1 db, ± 5° in phase and ±0.01 Hz in frequency of the sinusoidal voltage. It will be seen that corresponding axes (e.g., G_{θ_D} and G_{θ_M}) are reasonably well matched. This has been done in order to achieve smooth distortionless response in the difference of the two actuators' positions. The reason for doing this will be discussed later.

Because the motion system is floor-mounted, its maximum bandwidth is higher than that of the visual display. Its dynamic response therefore was degraded to match that of the less stiffly mounted visual display. The potential maximum bandwidth of the motion system with the proper compensation is about 15 Hz (see Figure 20). Therefore, it will be seen that in the case of some of its actuators, no compensation is required to achieve the 2 Hz bandwidth exhibited by the visual display.

The required compensation is expressed in terms of the ratio of velocity to position gain for each actuator. If the commanded actuator position is denoted by, for example, θ_D, then the command voltage $\hat{G}_{\theta_D}$ may be expressed by

$$\hat{G}_{\theta_D} = K_p \quad \theta_D + K_v \quad \dot{\theta}_D$$

In transfer function form,

$$\hat{G}_{\theta_D}(s)/\theta_D(s) = K_p \left[1 + (K_v/K_p)s\right]$$

K_p (position gain) is the slope of the input calibration plot for the actuator (Figure 7). K_v, the velocity gain, may be easily calculated from the value of K_v/K_p given in each frequency response plot corresponding to that axis (Figure 19, in this case). The inverse, K_p/K_v, may be recognized as the break frequency (rad/sec) of the lead network which comprises the compensation.

Velocity Error

Some measurements of velocity error for the visual display have been taken and are presented in Figure 25. Velocity error here is defined as the difference between commanded and actual actuator position under steady-state conditions when a ramp position command is applied. It is generally a function of the ramp input slope. For a type 1 servo, it is a linear function of the ramp input slope; for a type 2 servo, it is zero. Inspection of Figure 25 shows generally the characteristics of type 1 servos with the exception of the G_{X_D} servo, whose error is zero. The errors are presented in volts to facilitate ready comparison with new measurements. The equivalent voltage/dimension relation is also shown. These errors are important for the actuators shown and will be discussed further. The approximate slopes of the velocity error curves are tabulated in Table VI for comparison.

TABLE VI. VISUAL DISPLAY STEADY-STATE POSITION ERROR/VELOCITY (SEC)

Actuator	Error (Ft/Ft/Sec or Sec)
G_{X_D}	0
G_{Y_D}	0.009
G_{Z_D}	0.038
G_{Ψ_D}	0.022 Deg/Deg/Sec

SOUND GENERATOR

The sound generator consists of a control console and two AR-5 high-fidelity speakers. The console contains eight variable-frequency oscillators and four different limited-band white noise generators as well as nine variable-gain amplifiers for attenuation purposes. Twelve buffer amplifiers and two summer amplifiers are also included. A small cartridge-type recorder is available for invariant forms of sound. All power supplies and patch panels are carried in the control console. A photograph of the control console is shown in Figure 26.

Design

The aircraft sound system except for the external speaker system is entirely self contained in an Emcor type cabinet enclosure. The system contains its own precision DC power supplies so that, except for external AC plug-in, it is an entirely independent sound simulator. The circuit design is based on standard general-purpose circuit cards which utilize solid-state components. The use of standard cards provides the utmost in design flexibility. The cards are linked via a patchboard panel so that the user can readily vary the way the standard cards are connected and thus generate widely diverse types of sounds. While the sound system can be manually operated by manipulation of control potentiometers (easily accessible on the front panel), its basic intent is that the sound outputs be varied by computer analog inputs for which the circuit cards are designed. The output signals can be patched into either one of two PAT-4 Dynaco Stereo Pre-amplifiers which drive two 120 Dynaco Stereo Power Amplifiers. Each power amplifier can in turn be patched into either an external AR5 Speaker System or a locally contained monitor speaker system. Provisions have also been made to insert tape-recorded sounds into the sound system. This might include an actual starter motor sound prior to the start of engine sound.

Sound Description

The aircraft sound system is capable of creating reasonable facsimiles of the following aircraft sounds:

Aerodynamic Hiss: This sound is a high-frequency white noise, the loudness of which is a function of airspeed.

Exhaust I & II: These jet engine exhaust sounds are two separate lower frequency bands of white noise. Exhaust II is lower than Exhaust I. The loudness is a function of engine throttle and torque.

Runway Rumble: Runway rumble is the lowest frequency of white noise available, the loudness of which is a function of aircraft weight on wheels and ground speed.

Reciprocating Engine Exhaust: This sound can be simulated by suitably combining either Exhaust I or Exhaust II with square wave voltage-controlled oscillators and voltage-controlled variable-gain amplifiers, coupled with transmission whine generated by higher frequency voltage-controlled oscillators.

Rotor Prop Sound: This sound is similarly generated as the reciprocating engine exhaust except that Exhaust I is used in combination with lower frequency voltage-controlled oscillators.

Jet Engine Sound: Jet engine sound is a combination of continuous high-frequency and low-frequency white noise, together with transmission whine provided by the voltage-controlled oscillators.

Figures 27, 28, and 29 contain sound generator frequency calibrations for three of the available variable frequency oscillators. Note the nonlinear nature of the data at low frequencies.

SIMULATOR PAST USES AND PROJECTED FUTURE USES

From the time of its completion in April 1967, the rotational simulator has been used to study a variety of flight and flight-related problems. A summary of the problems and the vehicles is given below:

1. Early validation studies for hovering and low-speed flight using the NASA - Bell X-14A VTOL vehicle.

2. Generalized VTOL hovering and low-speed flight studies of handling qualities.

3. Later validation studies for hovering and low-speed flight using the NASA - Bell X-14A VTOL vehicle. These studies included a motion base evaluation.

4. Preliminary studies of STOL approaches and landing using a generalized STOL transport vehicle.

5. Error effects study of the NASA - Bell X-14B variable-stability system.

6. Flight control and guidance system development using the CH-47C helicopter (in conjunction with Boeing-Vertol).

7. Evaluation of the use of the rotational simulator as a helicopter pilot trainer using the Bell OH-13G helicopter.

8. Additional flight control, guidance, and manipulator subsystem development using the CH-47C helicopter.

In addition, a few purely physiological "ride" type tests have been conducted for the purpose of determining the relevant human motion perception.

A cursory examination of the above problems will reveal that most of the work on this simulator has been done using flight velocities of 100 knots or less, close to the ground. A sizable portion has been conducted with large vehicles where pilot station distances to the center of gravity were also large.

There are several technical factors which cause the research to center on these regimes, and they are discussed as follows. First of all, the very good outside visual environment display makes it ideal for situations where strong ground references are required such as landing and takeoff

and low-altitude helicopter type operations. Second, the available maneuvering space and attitudes constrain the speed. Much of the work has been conducted on the 750 to 1 transparency, which has a useful planform area of a rectangle 3000 feet to a side. With the present interface mechanizations, the maximum bank angle achievable in a coordinated turn is 20 degrees. A simple calculation will reveal that circular flight paths with a radius of 1500 feet and a bank angle of 20 degrees occur at speeds of about 80 knots.

Third, the limited motion-base capability will not produce a faithful enough representation of the pertinent motion stimuli characteristic of high-speed flight. Also, when large pilot station offsets from the center of gravity are present, the motion stimuli resulting from rapid attitude changes cannot be adequately represented and therefore the simulation results become questionable. The problem of requiring the simulation of sustained normal acceleration is of course not understood at this time, nor is the simulator capable of producing these sustained normal accelerations.

Future uses of this device will probably continue to center on problems of low-speed vehicles maneuvering close to the ground. These problems will most likely be with helicopter configurations of the advanced type, i.e., compound, stowed rotor, etc. The last two programs which used the simulator included mechanizations of ground contact dynamics. It is very likely that future uses will include sophisticated ground contact analysis, particularly if the motion base capability is increased.

It is possible to use the device to represent instrument approaches, and as such automatic or partially automatic flight problems will most likely be investigated. These problems could include those of a space shuttle craft during instrument approach and landing. The inability to represent sustained normal acceleration (the case during flare-out) may not compromise the validation of such a simulation.

The small attitude capability of the device may still be adequate to examine the Mars landing mission. Unlike the lunar landing mission, some atmospheric effects will be present which may prove troublesome in the early design of a Mars landing craft. The device could be used to explore a combination of aerodynamic and reaction type control moment generators for use in guidance system analyses.

With the advent of the high transfer training simulator, a variety of possible uses exists. Certainly, many studies will be performed which seek to define simulator requirements for training and training effectiveness. Automated teaching will be explored, and a variety of new display devices or information processers will be investigated. Research for a driving simulator could be performed using the device. Problems peculiar to the semiautomatic automobile could be easily investigated.

Without a doubt, simulators will prove to be valuable in redefining and reassessing the man-machine integration problem in the next two decades, and this simulator could make its contributions also.

SIMULATOR VALIDATION

VALIDATION DATA

Simulator validation is defined here a that process which results in evidence that the approximations offered in the mathematical representation and interface computations, and inherent in the stimulus generator (the simulator hardware), do represent the situation being simulated to a definable degree of accuracy.

The extent to which a user wishes to validate his simulation may vary from zero to an extreme level. The level is obviously related to the objective or purpose of the simulation. Three general classifications are identifiable.

The first is the purely exploratory simulation where little is known about the vehicle or its operating environment and where it makes little sense to study the validity of the stimuli offered to the pilot when the factors responsible for them are largely unknown. The second is the situation where a known vehicle is to be modified or a new design is being developed which is not too different from an existing one, where much useful information can be obtained by attempting to validate the known vehicle. When this has been done, changes in the interface coefficients may be made which may be based upon reasonable assumptions and which will result in high confidence that the results will be as valid as those from the known vehicle. The third is a pure validation study where practically all of the time is spent examining the pilot-simulator interface with very little energy expended in verification of the mathematical representation of the vehicle.

Since the second situation describes the case where the simulator is used as a design tool, it is the most prevalent example. Unfortunately, the pressures associated with generating a design often preclude a reasonable validation effort, and programs of this kind often result in validation efforts which seldom exceed 10 to 20 percent of the total program test time.

METHODS OF VALIDATION

There are three basic ways in which a simulator may be validated, which are based upon the degree of pilot participation. They are as follows:

1. Subjective, where the opinion of the pilot is the sole indicator of fidelity. Usually a rating system is used and task instructions are included as part of this rating system.

2. Objective, where the pilot is considered to be only an element in the system and therefore does not perform any analysis functions. The pilot may be physically an element, or represented by a mathematical model. Numerical analyses are used to generate a fidelity index, and statistical methods are commonly employed to assess pilot variations. "Goodness" criteria are often used which are based upon pilot-vehicle performance parameters.

3. Combination of Subjective and Objective, where the best utilization of the pilot and numerical analyses is made. Pilot opinion data are kept relevant to the pilot's capability. Maximum use of the computer is made to facilitate numerical analyses that complement and hopefully correlate with the pilot opinion data.

The above classification describes the problem of validation by using the degree of pilot participation as an index. This, however, is not the only factor that must be considered. Analysis techniques are available which can be used to complement the pilot opinion data. It is reasonable to expect that when the quantitative indices indicate a good or high degree of fidelity, the pilot opinions will reflect this also; therefore, the two forms of data tend to complement each other.

The following describe several validation methods which detail the above classification. They may be used individually or simultaneously to effect validation.

1. Pilot opinion rating.

2. Simple time history comparison from the pilot-vehicle and pilot-simulator systems.

3. Time-dependent random data analyses of selected variables of the pilot-vehicle and pilot-simulator systems to determine the degree of static and dynamic equivalence.

4. Pilot modeling techniques using random data analyses to establish when the pilot models for simulator and flight are equivalent.

5. Measured/computed stimuli analyses without physiological assumptions using random data analyses techniques.

6. Measured/computed stimuli analyses with physiological assumptions regarding the relevant stimuli required based upon related physiological studies and employing random data analysis techniques.

The methods are listed in order of increasing difficulty in execution and are discussed below.

1. Pilot Opinion Rating

Examples of pilot rating systems are common in the literature and will not be discussed here except to say that special types of rating systems are usually required depending on the task and the nature of the simulation. Together with adjectives describing the ease with which a task could be performed and the degree of accuracy or precision attained, these rating systems are required to help the pilot make comparative judgements regarding similarity to the corresponding flight condition from the point of view both of environment and of vehicle characteristics, whether known or unknown. It is extremely necessary to motivate a highly skilled test pilot in working with this method. He must be articulate, perceptive, curious, and above all, cooperative or else this method will yield less than desirable results.

2. Simple Time-History Comparison

A simple comparison of time histories from the pilot-vehicle system with those from the pilot-simulator system. Task commands are given to the pilot, and he executes them in both the simulator and the aircraft. In this case the existence of the aircraft is assumed, and this type of validation is useful for problems involving vehicle modifications. Data acquisition and processing requirements are of course minimal.

3. Random Data Analyses

Random data analyses of selected time histories from the pilot-vehicle system and the pilot-simulator system. The purpose of this type of validation is to establish the degree of static and dynamic equivalence achieved between the pilot-vehicle and the pilot-simulator system. Under the assumption that both systems are represented by ergodic stationary random processes, many interesting analyses are possible which include auto and cross correlation functions, power spectral density and cross

spectral density distributions, and probability and joint probability density functions. Related analyses include coherence functions and of course the standard mean value and root-mean-square values, etc. Again the existence of the aircraft is assumed. Data acquisition and processing are extensive.

Certain inherent advantages are possible, however; for example, the difficulty in sequencing maneuvers shows up as a difficulty in time-alignment of the two sets of time histories. The fact that random analyses of time histories implies a time dependency is the key to this problem, in that only a limited time (or frequency) domain is important to the problem. The spectral and correlation analyses are capable of addressing the problem at its most sensitive point. For example, in assessing or determining rotational motion effects, the bandpass of the pilot's semicircular canals (Ref. 2) appears to be the dominant domain of interest, and analyses in this range will yield fruitful results. Vehicle linear motions on the other hand occur at frequencies from zero to those of the rotational motions. The greatest portion of this energy, however, is found at very low frequencies, and analyses at low frequencies are meaningful. Again, the existence of the aircraft is assumed, and it is helpful if the same pilot is employed for all analyses.

4. Pilot Modeling Techniques

Pilot modeling techniques are designed to determine the applicable pilot model for a particular pilot-vehicle and pilot-simulator system and to demonstrate its use. If the simulator pilot model can be shown to be equivalent to the flight pilot model, the simulator is valid. Also, the relevant pilot factors are determined and statements can be made regarding the usefulness of these factors. Unfortunately, the forms of the models must be assumed or based upon models of the nervous system. The method uses measurements of system input and output variables and thus requires a knowledge of the input itself, which is usually in the form of task commands in the pilot's brain for the so-called "open-loop" tasks and special display information with associated drive equipment for the "closed-loop" tasks. For this method, therefore, only closed-loop tasks such as tracking can be handled easily. An important aspect of this method is that it is capable of producing information which could be used directly in the interface computation design.

5. Measured/Computed Stimuli Analyses Without Physiological Assumptions

Measurements of simulator variables such as acceleration may be taken and correlation analyses conducted with the same variable predicted by the computer. If a perfect correlation can be shown, the simulation is of course perfect. This will obviously never happen at all times; therefore, a tool is created which allows the user to examine a measure of fidelity at any time period he wishes. These indices may then be related to the effectiveness of the simulation; for example, relating the index for the period of the time sample to the task or an interface coefficient chosen for that time period. It is obvious that the method by itself is not able to predict solutions to deficiencies.

6. Measured/Computed Stimuli Analyses With Physiological Assumptions

This method also provides design information for the interface computation. In an example of this method, estimates of the relevant sensory perception are made using theoretical or measured physiological data. An interface mechanization is then designed which meets the requirements above and which also satisfies the constraint requirements such as motion travel limits, etc. Measurements are then made of the appropriate variables and compared with the corresponding computed quantities. Random data analysis techniques may be employed to determine if the simulator is reproducing the variables with the required accuracy. In this instance, cross-spectral analyses and/or cross correlation techniques are particularly useful in establishing that the simulator is reproducing the relevant stimuli at the proper time. A knowledge of the relevant sensory perception is required. Some of these data are presently available (reference 2); the rest must be assumed or data generated by related tests. Testing of this kind has been reported in reference 2. An example of the methods 1, 3, and 6 is shown in reference 3 for a pure validation study.

In this example, flight data were available for two specific tasks. The same pilot participated in all tests and offered comments. The primary analysis was the power spectral density analysis. Some data which indicate stationarity were taken. The slight periodicity of the data for one task was noted.

The reader may ask at this point if there are any other validation methods besides the ones described. There probably are, and a possibility which was not mentioned is the equivalence of training. In other words, the hypothesis is that when the transfer of training to an actual vehicle from that in a training simulation is 100%, this is sufficient proof of the validity of the simulation. Unfortunately, this is not always true, and it is recognized that exactness in simulation is not a requirement for training simulators and that it should be possible to obtain unproportionally high transfer without a high degree of realism.

In Table VII, validation methods are suggested for various classes of simulation as previously defined. The suggestions are based on observations of the progress of many simulations. The table is intended to help clarify the concept of validation and to assist in the selection of a method which fits well with the experimental design.

TABLE VII. SUGGESTED VALIDATION METHODS

Method	PURPOSE OF SIMULATION AND PERCENT EFFORT FOR VALIDATION			
	Exploratory Study < 10%	Engineering Research and Development, Training Research < 50%		Simulation Research < 90%
		Unknown Vehicle	Known Vehicle	
1	X	X	X	X
2			X	X
3			X	X
4		X	X	X
5			X	X
6	X	X	X	X

EXPERIMENTAL DESIGN

RATIONALE

The experimental design is a procedure which allows the intelligent selection of subsystem components and their performance for a simulation using the rotational simulator. The components to be considered are the following:

1. Visual display subsystem
2. Motion base subsystem
3. Cockpit controls and displays subsystem
4. Sound generator subsystem
5. Auxiliary station subsystem
6. Measurement/analysis/record-playback subsystem

Below is a discussion of the factors which must be considered in determining the required subsystems and their characteristics:

1. A precise definition of the desired flight tasks and a reasonably good estimate of the expected flight paths with the associated vehicle attitude and translational velocities as a function of time.
2. The proportion of the flight task to be conducted by visual outside reference and by visual outside and/or instrument reference.
3. The frequency content of the maneuvers expected including, if possible, estimated closed-loop bandwidths of the rotational motions and the apparent forces at the pilot's station including the vibration effects.
4. An estimate of all sounds audible to the pilot which may either be correlated or uncorrelated to vehicle motion or control inputs.

5. The selected cockpit arrangement of displays and manipulators. Static and dynamic manipulator force characteristics.

6. The auxiliary station arrangement for the observer/monitor/director/instructor including displays, manipulators, switches, etc.

7. The desired validation method.

8. Definition of measurement/analysis or recording-playback procedures.

Reference to these factors are made in the following sections.

SELECTION OF VISUAL DISPLAY CHARACTERISTICS

Transparency Scale

The maximum scaling limits of the problem will be determined by the initial two factors (Factors 1 and 2) mentioned in the previous paragraph. The instrument reference flight path will dictate the maximum limits. Visual display limits are taken from the visual reference desired flight path size and associated vehicle steady state attitudes. Steady-state attitudes are required here because of the integrated method used to drive the visual display and the motion base. This will be discussed more fully later. If the earth position integrators are limited to the flight path "dimensions" for instrument flight, an infinite flight area is still possible under instrument conditions if a knowledge of precise position is not desired. When the aircraft reaches the visual display limits, a light mask may be actuated which will instantly darken the ground scene. The sky projector light will remain lit, however, and the resulting visual scene will closely resemble flight over a ground-obscuring haze layer during twilight hours.

Although no attempt has yet been made to represent night visual conditions, it does not appear difficult. An opaque paper mask with holes of varying size representing lights on the ground may be laid on the transparency's lower surface. The point light will remain on while the sky projector lamp power is varied to represent lighting conditions from twilight to those of a dark overcast night.

Once the transparency scales have been chosen with the aid of Table I, the permissible position thresholds must next be considered. These may be found in Table II. The position thresholds must be compatible with the desired position sensing or position tracking performance. Specifically, this means that if the minimum position sensing capability associated with all the tasks for one transparency is determined, the threshold for that transparency must be no larger than one quarter of this value. If it is, the transparency scale must be lowered and the flight task modified.

From the expected translational velocity (Factor 1), estimates of position error can be made with the aid of Table VI, which contains measured velocity errors. If the task is such that perception of correct position is necessary, and an accuracy can be defined, the velocity error associated with each translational actuator (earth axes) must of course be less. This situation usually occurs only during high-speed operation where accurate spatial perception is usually not a requirement. If such position errors can be tolerated as being part of the total error generating system and only a knowledge of the instantaneous apparent position is required for apparent error analysis purposes, the translational actuator's feedback elements may be used to indicate the instantaneous apparent position.

The minimum ground height which can be represented by the visual display is the minimum vertical distance between the point light and the upper transparency surface multiplied by the transparency scale S. This distance is 0.2 inch when the light is near the perimeter of the transparency and somewhat larger when the light is near the center because of transparency sag. The sag is less for the circular transparencies (S = 550, 100) than for the square ones (S = 2000, 750). The sag has not been measured, but appears to be about 0.1 to 0.2 inch. It can easily be seen that at a scale of 2000 to 1, the minimum ground height at the center of the transparency is about 0.2 x 2000 = 800 inches or 67 feet.

It is not advisable to simulate heights which require distances between the point light and the upper transparency surface of less than 0.5 inch, because the visual display actuator movements (primarily the pitch actuator) occasionally excite an 8 Hz transparency bending mode with amplitudes of about ±0.01 inch. At a scale of 2000 to 1, this is an amplitude of ± 20 inches. At 100 to 1, it is ± 1 inch. These vibrations are readily apparent when the light-to-transparency distance is less than 0.5 inch and must be considered when selecting transparency scale.

Transparency Content

The four available transparencies are of course decorated as described earlier. The transparencies may be modified to include objects which enhance the pilot's ability to determine a stable visual environment. Usually, the adequacy of a transparency can be assessed by the pilot by allowing him to view it statically from the cockpit. It must be pointed out to the pilot that the available maneuvering area is less than that displayed, the difference being about 1 foot (real-world) along the perimeter.

When maneuvering near three-dimensional objects, it is possible to "collide" with them, and for this reason they are usually taped to the surface. Collision is caused by the point light source support housing contacting the object. To assess this possibility, simply examine the housing and view it as the simulated body of the aircraft being represented. With the pilot's eye center (a point halfway between the eyes) coincident with the point light source, it will be immediately seen whether or not a collision possibility exists. At a scale of 100 to 1, the housing (in the projected world) is about 40 feet long. It will be proportionately greater for the larger scale transparencies.

The frequency content of the maneuvers expected (Factor 3) must be examined in order to determine if the bandwidth of the visual display is adequate for the expected maneuvers. The inputs to the visual display translational actuators are related to the position of the pilot's eye center over the earth. The motion of the eye center will occur at frequencies of the vehicle's attitude motions when the pilot station is not at the center of gravity of the aircraft. Since the measured bandwidth of the translational actuators is about 1.8 Hz, the highest frequency which could be followed without incurring a phase lag of more than 20 degrees is 0.6 Hz.

This is not a factor for the pitch and roll actuators of the visual display because, again, of the way in which the drives for the visual display and the motion base are integrated. The pitch and roll actuators must follow inputs only up to about 0.2 Hz; therefore, the measured bandwidth of about 2.0 Hz is more than adequate. It is an important factor, however, for the yaw actuator. Because of the limited ($\pm$ 7°) yaw capability of the motion base, the visual display must follow the yawing motions of the aircraft. This actuator's frequency response is shown in Figure 21. Examination of this figure will reveal characteristics of a system with magnitude attenuation of 3 db with a phase lag of 60 degrees at 1.5 Hz. Therefore, it is not reasonable to expect the system to follow accurately (phase lags of less than 20 degrees) at frequencies of more than 0.65 Hz.

SELECTION OF MOTION BASE CHARACTERISTICS

Basis for Need for Motion

The question of the need for motion has not been fully resolved as yet. Many studies point out that its inclusion results in not only a better simulation but in some cases quantitative data which compare closely with flight results (reference 3). In some cases it is absolutely necessary.

This question will not be belabored here further except to hypothesize that the relevant human motion perceptive process appears to be the following:

1. Angular velocities are perceived directly in a frequency range of 0.4 to 6 rad/sec with some magnitude attenuation and phase shift. Estimates of angular position may be made from motion occurring in this range, but these estimates will become inaccurate (drift) with time if no other stimuli are present.

2. Forces acting on the pilot are the principal means of perception relating to translational motion. The perception of force will be combined with a knowledge of the flight environment to establish the stable frame of reference. This process is aided greatly by updating, using vision whether it be related to outside visual information or that from inside displays. For example, when "1g" conditions are known to exist, the perception of force is analogous to attitude with respect to the earth. When "1g" conditions do not exist as in a steady level turn or in pushover maneuvers, the perceived sensations are either disregarded or correlated with a knowledge of that particular environment to aid in the establishment of the stable reference.

The two classes of stimuli, rotational and translational, are integrated with visual stimuli in the higher association centers of the brain to produce a precise knowledge of orientation with respect to the selected stable reference, which includes velocity and probably acceleration information.

The above hypothesis leads to definite motion and visual requirements which are highly related. The relation is demonstrated by the nystagmus response, which has evolved to aid in the maintenance of an established stable reference in the presence of head movements. Therefore, one cannot speak about a good visual display and motion system separately.

Establishment of Motion Requirements

The requirements for motion system-visual display integration are drawn from the two statements above and are :

1. Rotational motion is required when the expected closed-loop bandwidth of the attitude control exceeds 0.4 rad/sec, whether the reference is outside visual or inside visual. Attenuated motion appears to be acceptable.

2. Rotational motions occuring above 10 rad/sec are classed as those relating to vibration effects, etc., and are perceived as modulated environmental stimuli.

3. Apparent force representation is required with minimum attenuation and phase shift from 0 to 10 rad/sec, the upper requirement for rotational motion.

4. Apparent forces occurring above 10 rad/sec are classed as those relating to vibration effects, buffet, etc., and are perceived as modulated environmental stimuli.

The required amount of motion can be determined from the expected vehicle motions and a knowledge of the filtering which satisfies the above requirements. Usually the filtering is compromised so that available motion travels are not exceeded and stimulus correlation begins to deteriorate. This will be demonstrated by the validation effort.

Suggested filtering is shown in the "Interface Mechanization" section.

DETERMINATION OF COCKPIT CONTROLS AND DISPLAY SUBSYSTEM CHARACTERISTICS

Very little is required to ensure correct use of these systems. First, manipulator force feel measurements are needed in order to set passively (addition of a force servo system will modify these remarks) the desired characteristics using springs, dampers, magnetic brakes, etc.

Instrument and oscilloscope displays are not difficult to drive. Actual instrument lags must be measured and additional lag or lead introduced in order to reproduce the desired lag. Measurement of instrument lags is presently difficult because there are generally no feedbacks to use and no visual measurement systems available. Fortunately, the instruments with noticeable lag (e.g., vertical speed) generally require an additional lag which can be easily set by eye.

An annoying factor which must be avoided is the large transients which usually saturate the instruments when the record-playback feature is employed. This is discussed in the section dealing with recording procedures.

DETERMINATION OF SOUND GENERATOR SUBSYSTEM CHARACTERISTICS

A spectral analysis of sound pressure level at the pilot's station (Factor 4) is extremely helpful in determining the sound generator components that must be used. These data, however, are not the only requirement. When the spectrum has been synthesized and fitted with the outputs of the proper combination of voltage-controlled oscillators, gates, and limited-band white noise generators, the ear is still the final judge and pilot comment must be solicited to make the final adjustments.

Synthesis of aircraft sounds is not difficult in practice. Helicopter rotor noise is provided by a white noise generator triggered by a gate which is controlled by a voltage-controlled oscillator where rotor frequency (or multiples related to the number of blades) is equal to generator output frequency. Reciprocating engine sound may be generated in the same way except substituting cylinder firing frequency for rotor frequency and considering the effects of harmonics. Aerodynamic noise is limited-band white noise. Turbine and transmission sound can be represented by narrow-band white noise generators or a few voltage-controlled oscillators with either square or sine wave outputs depending on the desired harmonic content.

Two speakers are available (it makes no sense to conduct all the sound impulses to the pilot's headset without considering the attenuation properties of the headset and the fact that some sound is transmitted through the skull), which can be used to represent some of the directive properties of sound, i.e., rotor sound from the ceiling-mounted speaker, and engine sound from the one mounted either fore or aft of the cockpit depending on the engine location in the aircraft. The nonlinear input characteristics of the sound generator elements must be considered in applications where a wide range is desired (see Figures 27, 28 and 29).

DETERMINATION OF AUXILIARY STATION SUBSYSTEM CHARACTERISTICS

If an auxiliary station is required, the comments regarding the cockpit subsystem apply with the information of Factor 6. In addition, consideration must be given to the possible location of such a station. The platform immediately behind the cockpit may be used for this purpose. Care must be taken to ensure that modifications do not create an interference problem that could result in collision of the transparency carriage with the occupant of the auxiliary station.

Another important consideration is the quality of logic signals generated at the station for use in controlling various functions of the computer. Noisy logic signals can easily confuse a nand gate and cause it to malfunction. Either noise suppression techniques or relay systems must be employed to effectively operate the logic elements in the analog computers.

The last factor to be considered is the lack of motion stimuli of the observer's station and the fact that the visual scene is presently less correct to an observer at this station than to the pilot in the cockpit. This is due to the distance between the observer's eyes at the rear platform and the pilot's eyes. It results in mainly a position and higher derivative distortion of all objects viewed out the sides of the aircraft when the observer is directly behind the cockpit, and more complex distortion when he is not.

DETERMINATION OF MEASUREMENT/ANALYSIS/RECORD-PLAYBACK SUBSYSTEM CHARACTERISTICS

Generally, feedback signals are monitored to ensure that correct following by all the servos has been achieved. Since there are eleven hydraulic actuators in the visual display and motion subsystem, a fair percentage of the available recording capability would be used up.

The feedback information is generally not relevant to the problem, and it is suggested that six more relevant measurements be made instead. These are the three body axes accelerations and the three body axes rotational rates. Three orthogonally mounted accelerometers and rate gyros are mounted on a platform attached to the rear of the cockpit. Measurement of their outputs with their display next to the corresponding computed accelerations and body rates will prove to be most helpful during the simulation. This is of course a requirement for validation methods 5 and 6 as discussed earlier on page 19. No calibrations of these sensors are included in this document because it is strongly suggested that a calibration be made just prior to their use. The accelerometers are of course not mounted at the center of rotation, and consequently errors will be introduced which must be accounted for.

If special use of the actuator's feedbacks is desired, they can be used without affecting their performance provided the signals are isolated with buffer amplifiers.

As will be brought out in the next section, the apparent attitude seen from the cockpit is the difference between the motion base attitude and the visual display carriage attitude. If feedback measurements of the apparent attitude are desired, these feedbacks must be summed correctly. This is also discussed in the next section.

The record-playback feature which has been used successfully with this simulator is extremely useful in photographing the apparent motions and in demonstrating, documenting, and analyzing maneuvers. The technique consists simply of recording the total actuator input voltage and arranging to feed, by the use of switches, the tape reproduction of this signal to the actuator during playback. A 10-rad/sec first-order low-pass filter is required to suppress playback noise. Instrument readings may be reproduced in this manner, and more than one tape deck (14 channels each) can be used if synchronization can be achieved to an acceptable degree. A calibration voltage is required which is usually the reference voltage.

The circuit used to accomplish this is shown in the following sketch.

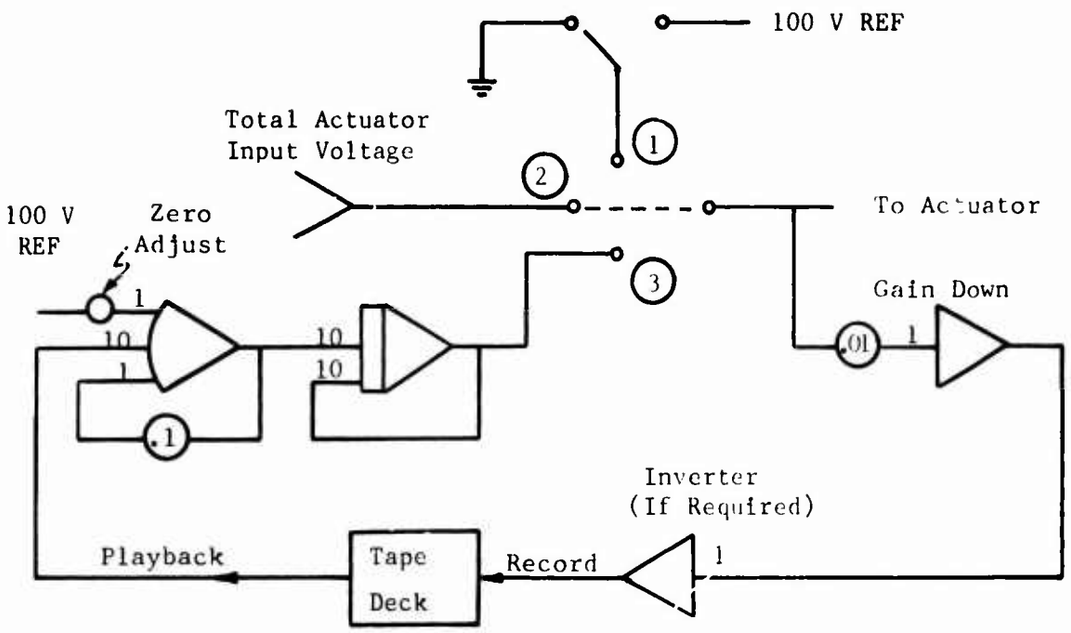

SWITCHING FUNCTION

(1) Calibrate

(2) Record

(3) Playback

To use the technique, simply record zero and the reference voltage on the tape prior to recording, and then record. To play back, simply reproduce the zero and reference calibration voltages, and then introduce the desired record to the actuators. Usually only one calibration at the beginning of the day is required.

The mechanization section discusses the method further regarding time scaling for photography. Photography is presently accomplished by recording at 60 inches per second and playing back at 1-7/8 inches per second. By photographing at one frame per second (necessary because of the low light level) and operating the processed film at normal speed (24 frames per second), the visual scene is reproduced at 3/4 real time (or 1 1/2 times real time if playback is at 3-3/4 inches per second).

The deficiency in time scaling is related to not being able to record correctly actuator rate inputs for compensation purposes because two tape channels per actuator would be required.

For real time applications, however, the method is excellent and greatly facilitates voice and data synchronization with the maneuvers. Analysis is greatly simplified as the tape may be easily electrically marked by an observer in the cockpit who is seeking to analyze only a specific maneuver.

INTERFACE MECHANIZATIONS

GENERAL RATIONALE

Two suggested interface mechanizations are presented in this section. The first (Mechanization A) is a simplified mechanization which requires the expansion of Euler angles in the gimbal order of the simulator and assumes that the pilot station is at the vehicle's center of gravity.

The second (Mechanization B) is an exact interface which utilizes the commonly used Euler angles (yaw-pitch-roll order) with provisions for transforming to angles for the gimbal order. It does not assume that the pilot station is at the vehicle's center of gravity.

The purpose of these mechanizations is to provide drive signals to the eleven hydraulic actuators of the motion base and visual display so that an effective representation of the vehicle is presented to the pilot. Instrument and control connections will not be discussed here, as their interface computations are straightforward and simple.

The mechanizations seek to offer the following stimuli to the pilot:

1. Rotational velocities with small attenuation and phase shift at frequencies from 0.4 rad/sec to 10 rad/sec.

2. Apparent force stimuli with small attenuation and phase shift at frequencies from zero to 0.4 rad/sec.

3. Accurate visual reference stimuli without appreciable distortion, attenuation, or phase shift from zero to 10 rad/sec.

4. Minimize false motion stimuli. Since the simulator motion subsystem lacks large translational motion (it has none laterally), the sensation of lateral and longitudinal acceleration will be produced by tilting with respect to the gravitational vector. This tilt will be called "postural tilt" in the following discussions because its intent is to maintain correct postural reflexes, and the semantics of the term are avoided.

The vertical degree of freedom of the motion base has been used with limited success in simulations where the pilot station is forward of the vehicle's center of gravity. Some attempts have been made to use the longitudinal (fore and aft) motion degree of freedom to help represent ground contact dynamics, but they have been largely unsuccessful to date.

It is strongly suggested that use of the translational motion base actuators G_{X_M} and G_{Z_M} be limited for two reasons. First, use of these motions severely limits the available motion travel of the rotary degrees of freedom, and second, their use increases the movements of the pilot's head with respect to the screen which causes visual distortion to increase.

They are, however, well suited to represent small-amplitude, high-frequency motions characteristic of a vibration or buffet environment. This is particularly true because these servo systems have a high bandwidth.

The general drive method is outlined in the next paragraph and is detailed in subsequent paragraphs.

Basically, the computed attitude of the aircraft is attenuated by a high-pass linear filter (a "washout") to an attitude which results in the correct lateral and longitudinal acceleration using only gravity components ("Postural Tilt"). The computed longitudinal and lateral accelerations which produce the "tilt" are attenuated by a low-pass linear filter. The sum is then introduced to the rotational degrees of freedom of the motion base. The purpose of the rotational high-pass filter is to minimize the false force sensations which follow from rotating in a gravitational field while not translationally accelerating. The low-pass filter minimizes the false angular velocity sensations which accompany rotation to an attitude which produces the desired sensations of longitudinal and lateral acceleration.

The remainder of the mechanizations are used to provide actuator compensation while avoiding open-loop or redundant integration and to satisfy the visual display assumptions. The visual display assumptions are included in the description of each mechanization.

MECHANIZATION A (Figures 30, 31, 32 and 33)

Rationale

A block diagram of this mechanization is shown in Figures 30 through 33. The first-order high-pass filters used for the rotational motions pass high frequencies to the motion system and low frequencies to the visual display. Filter time constants τ_p, τ_q and τ_r are related to the lower break frequency of the semicircular canals (the value generally used is about 2 seconds). The constants τ_x and τ_y are related to this also.

The nominal value is 3 seconds. The high-frequency gain constants K_q, K_p, and K_r should be set to unity. In the case of yaw, this is not possible due to the limited available motion (± 7°), and K_r is usually maintained at 0.2. These values may be reduced further without large deleterious effects when the task requires larger motions than are available.

When computing whether or not sufficient actuator travel or velocity and acceleration exists to represent the desired maneuver, simply compute the output of the interface from the input variables corresponding to the maneuver. In most cases the following is true regarding limits:

1. The maximum motion-base rotational acceleration in pitch and roll is equal to the vehicle maximum pitch and roll inertial rotational acceleration at the pilot's station.

2. The maximum motion-base rotational velocity in pitch and roll is equal to the vehicle's maximum inertial rotational velocity in pitch and roll at the pilot's station.

3. The maximum motion-base attitude is generally proportional to the maximum longitudinal and lateral accelerations and the maximum body rates at the pilot's station.

4. The maximum visual display attitudes are the maximum steady-state attitudes of the vehicle.

5. Because of the limited motion-base travel in yaw (± 7°), the maximum display angular acceleration and rates are equal to $1-K_r$ times the maximum vehicle heading angular acceleration and rate. The maximum motion system yawing accelerations and angular velocity are equal to K_r times the vehicle's maximum yawing accelerations and angular velocity.

More general statements may be inferred by examining the time response of the two types of linear filters employed in the mechanization.

The visual display linear actuators are driven by position and rate voltages representing the earth coordinates and the rates of the pilot's eye center. These coordinates and their corresponding rates are computed from the transformation of Figure 33. The transform has been approximated (see next section on "errors") and uses Euler angles expressed in the gimbal order of the visual display and motion base, (subscript 2), namely, yaw→roll→pitch (Case 4 on page 23 of Reference 4). The resulting earth coordinates are identified with the translational actuators of the visual display through the transparency scale constant S.

Generally, G_{X_D} is the north-south coordinate, G_{Y_D} is the east-west coordinate, and G_{Z_D} is the negative of the height coordinate. This nomenclature is arbitrary, however, and may be changed by the user if the transparency mounting orientation is also considered.

The added complexity of the yaw drive interface (Figure 32) is due to the continuous nature of the visual display yaw actuator. In order to prevent drift, sine-cosine potentiometers are installed on the yaw axis of the visual display and integrated into a position loop. The bandwidth of this loop is nominally set at 1 rad/sec by introducing the error signal, $\sin(\Psi_D - \Psi_{DF})$, to the G_{Ψ_D} actuator with unity gain. The rate bandwidth is extended to its maximum by the addition of a rate command signal. The result is a system with a rate bandwidth of 1.6 Hz with negligible drift. A continuous resolver is used to generate the sine and cosine of the heading angle from the heading rate.

The input variables required for this mechanization are the pilot station angular velocities and the apparent accelerations. The body rates are in the sense of the commonly used nomenclature p, q, and r. The apparent accelerations $\dot{U}_{OBS}$ and $\dot{V}_{OBS}$ require further clarification.

From Newton's second law, total external force is equal to rate of change of momentum, or under conditions of constant mass, mass times inertial acceleration. Symbolically,

$$\Sigma F \text{ (external)} = m (\dot{V})$$

When this equation is applied to a body of constant mass being accelerated near the surface of the earth, it becomes the following (longitudinal body axis frame of reference)

$$\Sigma F_x \text{ (aerodynamic)} + \Sigma F_x \text{ (gravity)} = m (\dot{u} - rv + qw)$$

The observed X body axis acceleration ($\dot{U}_{OBS}$) is, however, equal to

$$\dot{U}_{OBS} = \Sigma F_x/m \text{ (aerodynamic)} = (\dot{u} - rv + qw) - \Sigma F_x/m \text{ (gravity)}$$

This is readily apparent when one considers orbital (or free-fall) motion. The aerodynamic forces are zero and so is the apparent acceleration. In this case

$$m (\dot{u} - rv + qw) = \Sigma F_x \text{ (gravity)}$$

which is one of the equations governing orbital motion.

Under steady-state conditions during atmospheric flight,

$$m(\dot{u} - rv + qw) = 0$$

and

$$\Sigma F_x \text{ (aerodynamic)} = -\Sigma F_x \text{ (gravity)}$$

then

$$\dot{U}_{OBS} = -\Sigma F_x/m \text{ (gravity)}$$

which for level flight indicates that

$$\dot{U}_{OBS} = -\Sigma F_x/m \text{ (gravity)} = -g_x$$

where $g_x = -g \sin\theta_1 = -g \cos\varphi_2 \sin\theta_2$

It will be readily seen that for small $\dot{U}_{OBS}/g$, the steady state attitude of the simulator is the steady-state attitude of the aircraft.

The equations for all acceleration inputs are tabulated below for this mechanization:

$$\dot{U}_{OBS} = F_x/m \text{ (aerodynamic)} = \dot{u} - rv + qw - g_x$$

$$\dot{V}_{OBS} = F_y/m \text{ (aerodynamic)} = \dot{v} - pw + ru - g_y$$

$$\dot{W}_{OBS} = F_z/m \text{ (aerodynamic)} = \dot{w} - qu + pv - g_z$$

where

$$g_y = g \sin\varphi_1 \cos\theta_1 = g \sin\varphi_2$$

$$g_z = g \cos\varphi_1 \cos\theta_1 = g \cos\varphi_2 \cos\theta_2$$

Nominal (starting) settings for all coefficients of the mechanizations are given below :

$K_x = 1.0$	$K_y = 1.0$	$K_r = 0.2$
$\tau_x = 3.0$ sec	$\tau_y = 3.0$ sec	$\tau_r = 2.0$ sec
$K_q = 1.0$	$K_p = 1.0$	
$\tau_q = 2.0$ sec	$\tau_p = 2.0$ sec	

$K_{\theta_{M,D}}$, $K_{\varphi_{M,D}}$, $K_{\Psi_{M,D}}$, $K_{X_{M,D}}$, K_{Y_M}, and $K_{Z_{M,D}}$ are taken from the slopes of the static calibrations for these actuators (Figures 7 through 17). The velocity constants are computed as described in the section on frequency response data and required compensation, (page 8).

Errors for Mechanization A

Motion-base errors consist of the approximations of the Euler rates, the assumption that $\sin \Psi_m \approx \Psi_m$ and $\cos \Psi_m \approx 1$, and those due to placement of the filters after the computation of Euler rates instead of before. This results in perturbations of q and p not being precisely aligned with the body axes (fixed to the cockpit) for conditions where steady body rates are being applied. The equations for apparent acceleration also are for the case where the pilot station is at the vehicle's center of gravity.

The visual display errors are those due to the assumption that the cosines of φ_2 and θ_2 are equal to unity and second-order terms are negligible in the equations for the earth coordinates, X and Y. The equations are also for the case where the distance between the pilot's eye center and the center of gravity is zero.

More important, but less definable, visual display errors are those inherent in the assumption that the apparent attitude in the simulator is the difference between the motion-base attitude and the visual display attitude and is the result of the gimbal orders of both visual display and motion base being the same.

$$\theta_2 \text{ (apparent)} = G_{\theta_M} - G_{\theta_D}$$

$$\varphi_2 \text{ (apparent)} = G_{\varphi_M} - G_{\varphi_D}$$

$$\Psi_2 \text{ (apparent)} = G_{\Psi_M} - G_{\Psi_D}$$

The equations are not correct because of the finite quantity, [distance from the pilot's eye center to the point light source] ÷ [screen radius]. This is an error related to the distortion discussed in the section on the visual display principle and will not be elaborated further here.

Mechanization A should be used for small vehicles where the pilot station is near the center of gravity and the expected steady-state attitudes in pitch and roll are less than ± 20°.

The limiters shown in the mechanization are included only to avoid excessive resetting. They should be set to a few volts under the limit switch position (see static calibrations) to avoid resetting in transient conditions. When these limits are reached, the simulation is invalid and adjustments to the drive filter constants will be required.

MECHANIZATION B (Figures 34 and 35)

Rationale

In this mechanization, commonly used Euler angles expressed in the order yaw → pitch → roll (subscript 1) are generated and transformed into Euler angles in the gimbal order (subscript 2). The Euler rates in the gimbal order have been approximated here, but may be fully expanded if desired (reference 3). The expansions of the pilot's eye center velocities u_{p_e}, v_{p_e}, and w_{p_e} have also been simplified for a vehicle where the pilot's eye center is only forward of the vehicle center of gravity by the distance x_{p_e}. They also may be fully expanded using reference 4 if desired.

The pilot's eye center earth velocities $\dot{X}_{p_e}$, $\dot{Y}_{p_e}$ and $\dot{Z}_{p_e}$ are computed without approximation from the pilot's eye center body axes velocities u_{p_e}, v_{p_e}, and w_{p_e}.

The vertical actuator is shown driven by only the vertical component of motion due to pitching when the pilot station is forward of the vehicle's center of gravity.

The filtering used in this mechanization is identical to that of Mechanization A. The suggested additional constants τ_Z and K_Z are given below:

$$\tau_Z = 1 \text{ sec}$$

$$K_Z = 0.5/x_{p_s}\theta_2 \text{ (max)(ft)}$$

The summations for each actuator are not shown because they are made exactly as in Mechanization A. The pilot station observed accelerations are also identical to those of Mechanization A with the exception that the accelerations due to the pilot station offset from the center of gravity are to be added. These may be found in reference 4.

Two block diagrams of Mechanization B are shown in Figures 34 and 35. Figure 34 is a generalized diagram. Figure 35 is a detailed diagram of the yaw axis drive. In this case the display yaw actuator is used as an active computing element in that its feedbacks, $\sin \Psi_{DF}$ and $\cos_{DF}$, are used to help null the summing point forward of the limiter. By doing this, the computation is completed and the display reaches the correct position without redundant integration and with negligible drift.

Errors for Mechanization B

The assumptions of Mechanization A regarding the pilot's eye center and pilot station offset from the center of gravity were removed in this mechanization. The degree of representation of these effects is still at the discretion of the user.

The errors inherent in the assumption relating to the apparent attitude are retained. The computation of the earth coordinates of the pilot's eye center is exact, and the motion-base pointing error resulting from filtering after the Euler angle transformation is retained.

CHECKOUT AND OPERATION

Checkout

Checkout of both mechanizations is relatively simple. Static checking is done by placing initial conditions on all integrators and computing the static voltage on each summer. Dynamic checking may be done by simply placing the interface integrators into "compute" and recording the actuator drive voltages and feedbacks and comparing them with their corresponding theoretical values for actuator drive voltages.

A more meaningful dynamic check may be made by introducing control input steps and placing the whole system into "compute". Many points (or amplifiers) in the system may be recorded. However, the most meaningful are the body rates p, q, and r and the observed accelerations $\dot{U}_{OBS}$, $\dot{V}_{OBS}$, and $\dot{W}_{OBS}$. These quantities may then be compared with their corresponding computed values. During operation it is important to monitor the measured and computed body rates and accelerations.

It is stressed here that checks of all input and feedback calibration must be made prior to any linkup attempt. This is particularly true of the display yaw drive because an inadvertent high gain in the position loop will drive the yaw servo system unstable. The oscillation will not be harmful if the display yaw drive limiter is correctly set to a voltage which allows a maximum of ± 0.25 rad/sec. When a step display yaw rate of over this value is commanded, noticeable deflection of the supporting columns occurs.

Operation

It is desireable to place the system into "initial condition" before initiating the computation to ensure a smooth start. Doing this also allows the pilot to examine the initial conditions including sound and vibration. Several center stick buttons may be arranged for this purpose. Usually, three buttons are used, one for "initial conditions", one for "compute", and one for "reset". The point light source should be masked (it is solenoid actuated) during "fade in" to initial conditions and reset operations.

This is considered essential because of the tendency to induce pilot nausea when the pilot is shown large erratic movements with the visual display while not "feeling" these movements.

Operation of the playback tape feature requires starting of the tape deck first to avoid resetting the simulator actuators. When it becomes necessary to time scale a recording and a sufficient number of channels are not available to separate the actuator's drive signal velocity component from the position component, the velocity component must be switched out. This will of course limit the bandwidth of the visual display actuators to about 0.6 Hz. The motion-base actuators are affected only slightly because their required compensation is small.

LITERATURE CITED

1. STUDY OF POINT LIGHT PROJECTION SYSTEM COMPONENTS, NAVTRADEVCEN Technical Report 1628-1, March 1959.

2. Peters, R.A., DYNAMICS OF THE VESTIBULAR SYSTEM AND THEIR RELATION TO MOTION PERCEPTION, SPATIAL DISORIENTATION AND ILLUSIONS, NASA CR-1309, April 1969.

3. Sinacori, J.B., A STUDY OF V/STOL GROUND BASED SIMULATION TECHNIQUES, USAAVLABS Technical Report 70-16, U.S. Army Aviation Materiel Laboratories, Fort Eustis, Virginia.

4. Thelander, J.A., AIRCRAFT MOTION ANALYSIS, Air Force Flight Dynamics Laboratory Technical Documentary Report FDL-TDR-64-70, March 1965.

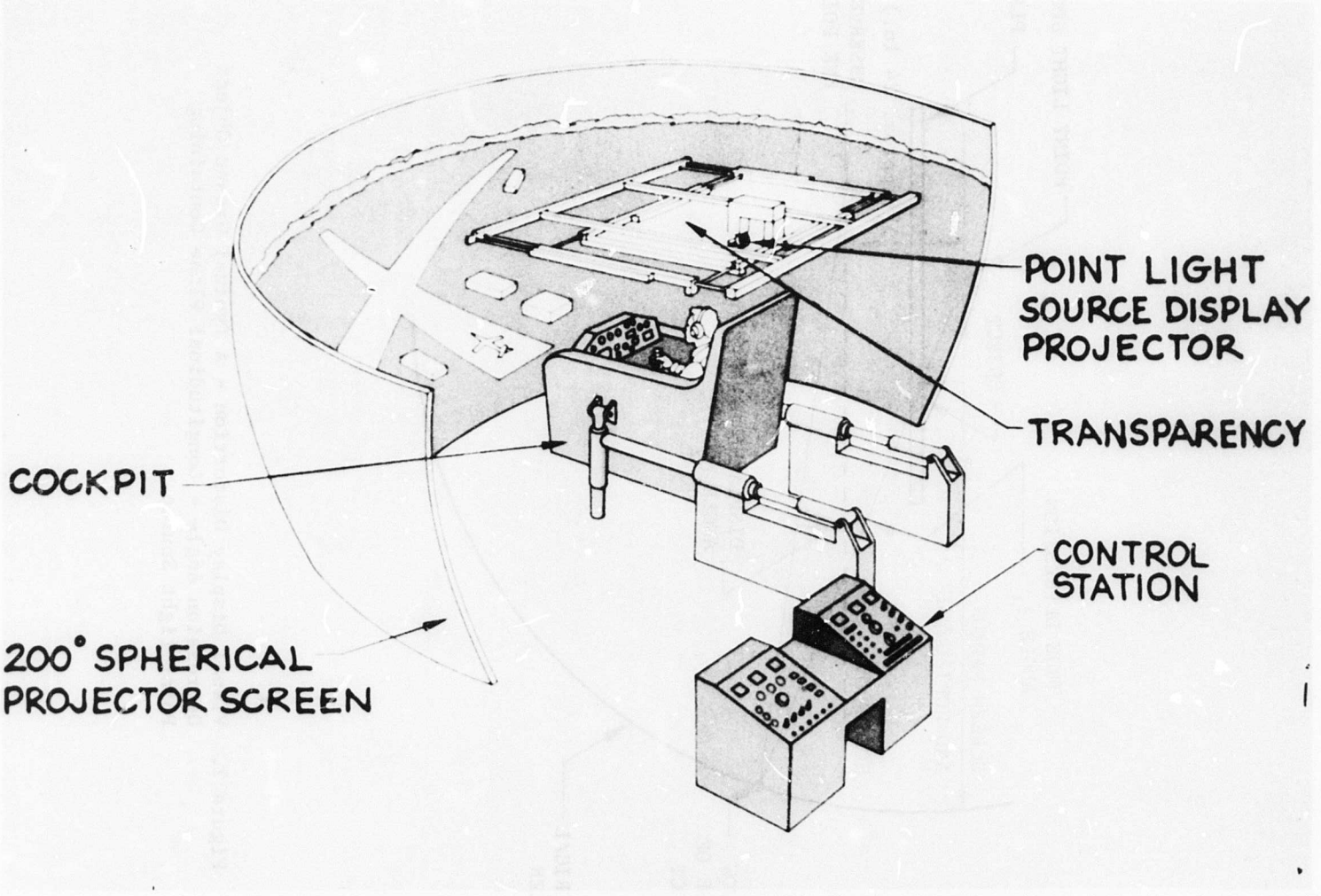

Figure 1. General Arrangement of the Rotational Flight Simulator.

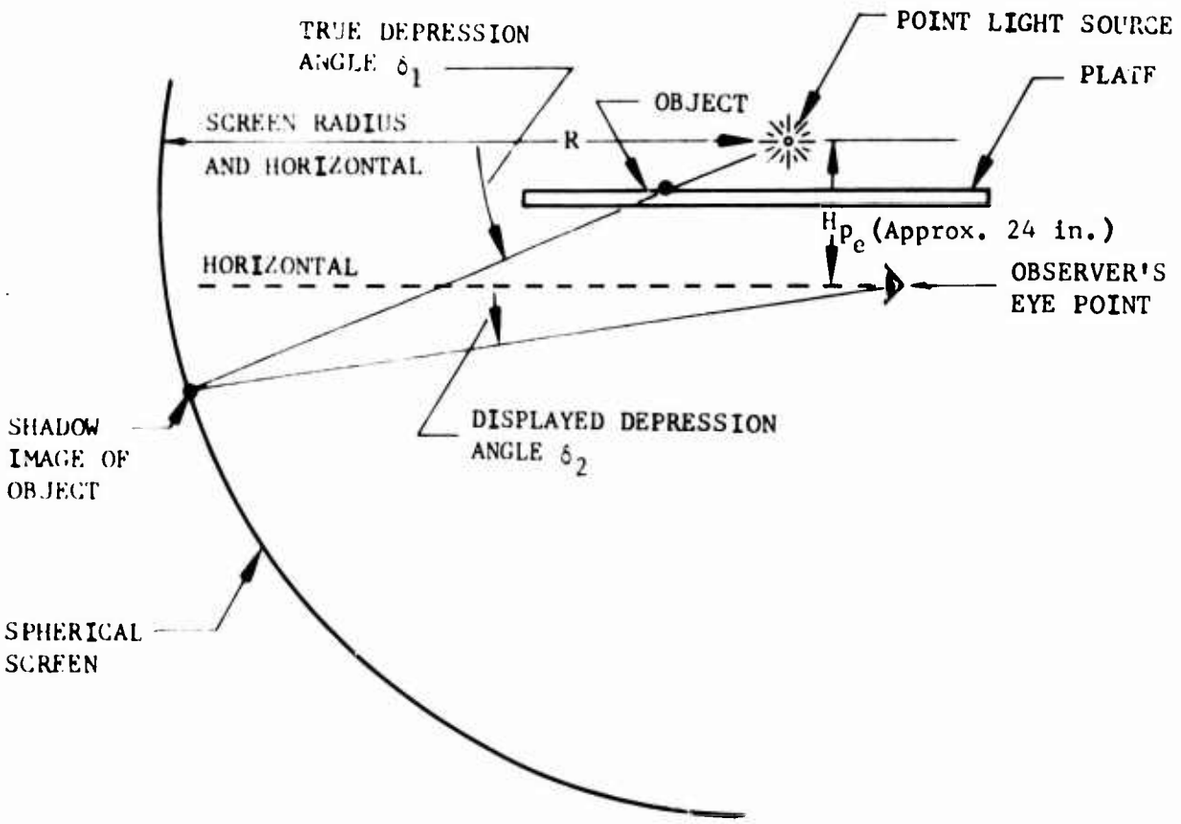

Figure 2. Visual Display Distortion - A Typical Ground Object Depression Angle - Longitudinal Plane Containing Point Light Source.

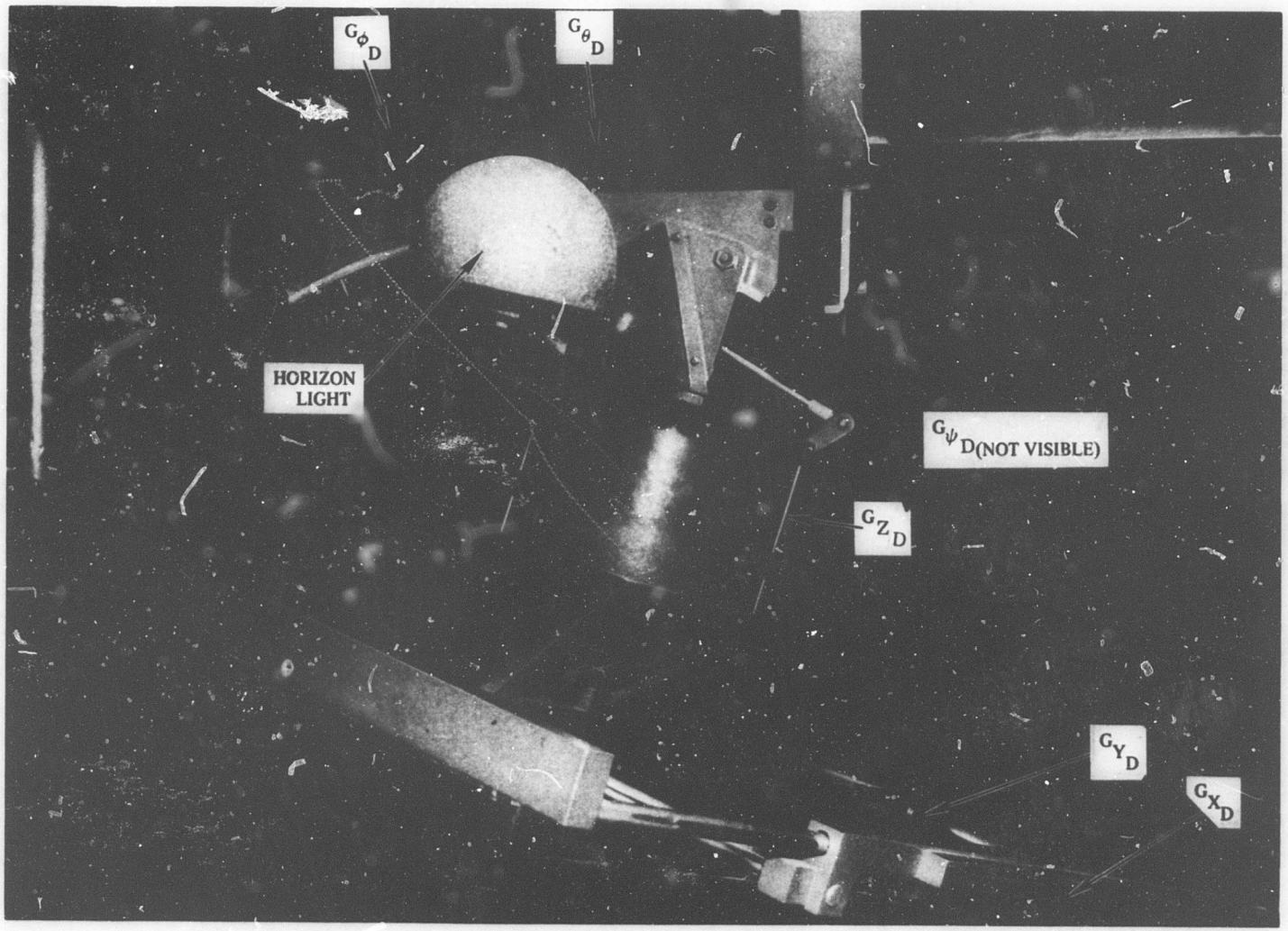

Figure 3. Visual Display Gimbal and Actuator Arrangement.

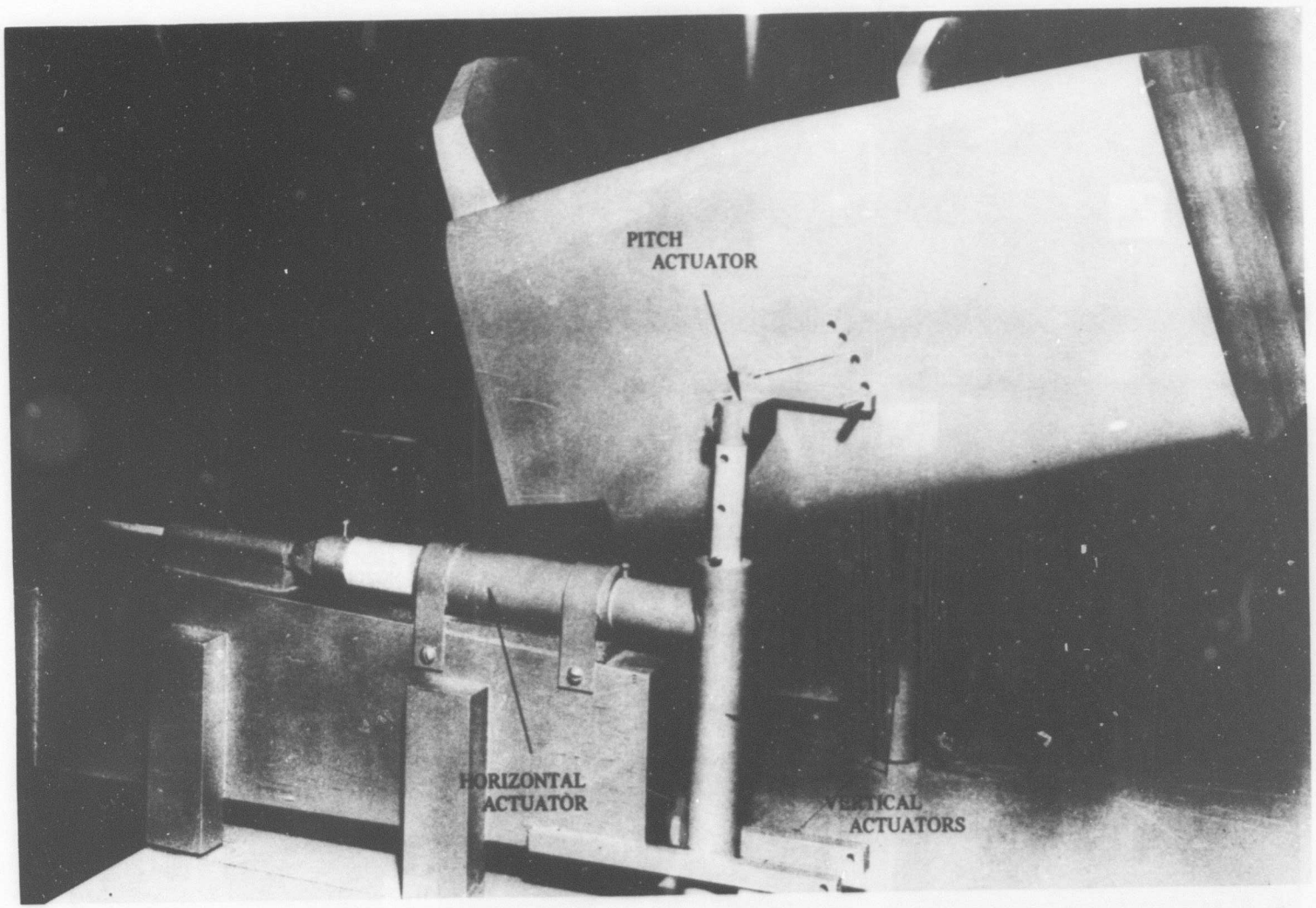

Figure 4. Motion Base Gimbal and Actuator Arrangement.

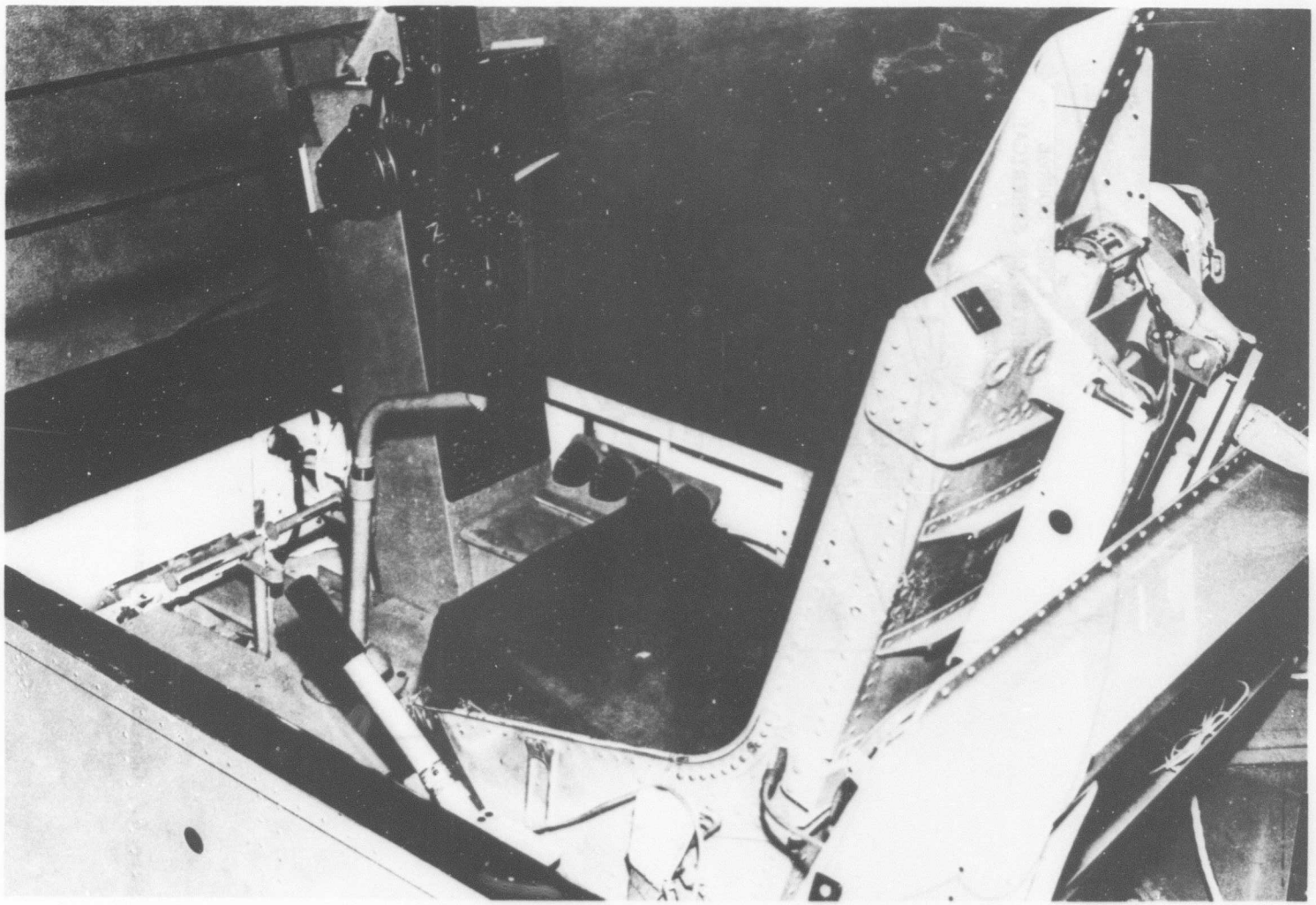

Figure 5. Cockpit Installation for the OH-13G Simulation.

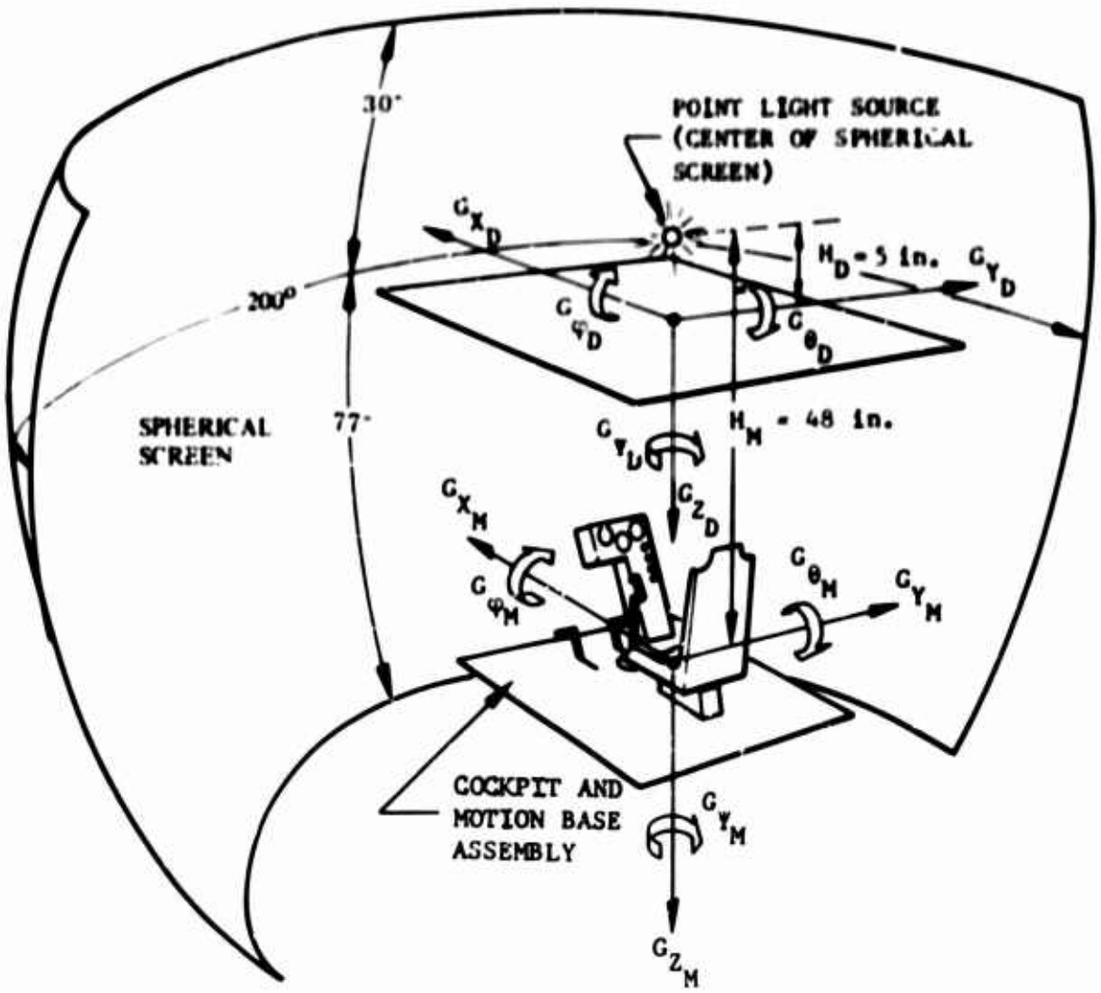

Figure 6. Coordinate Systems for the Visual Display and Motion Base.

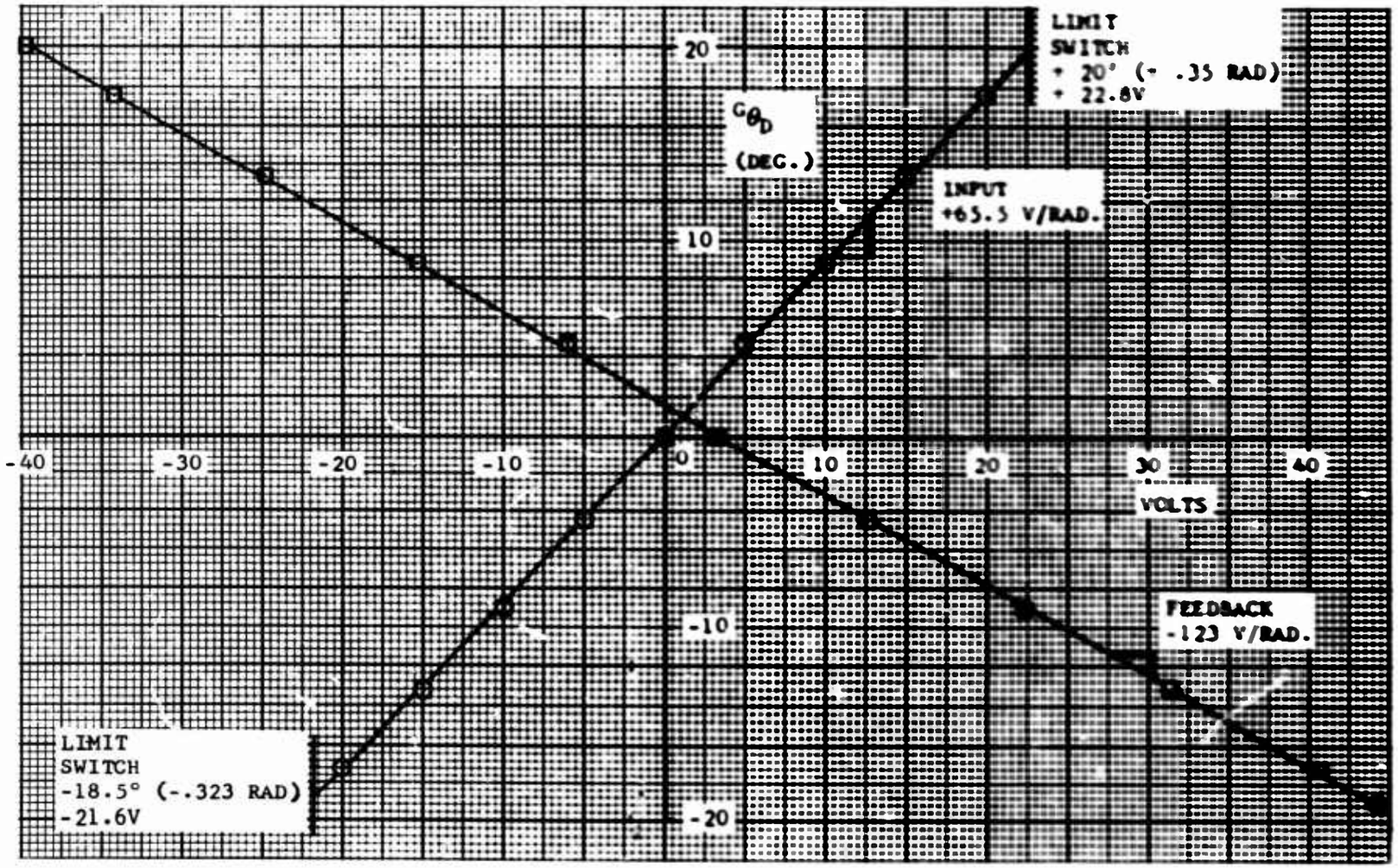

Figure 7. Static Input and Feedback Calibration for G_{θ_D}

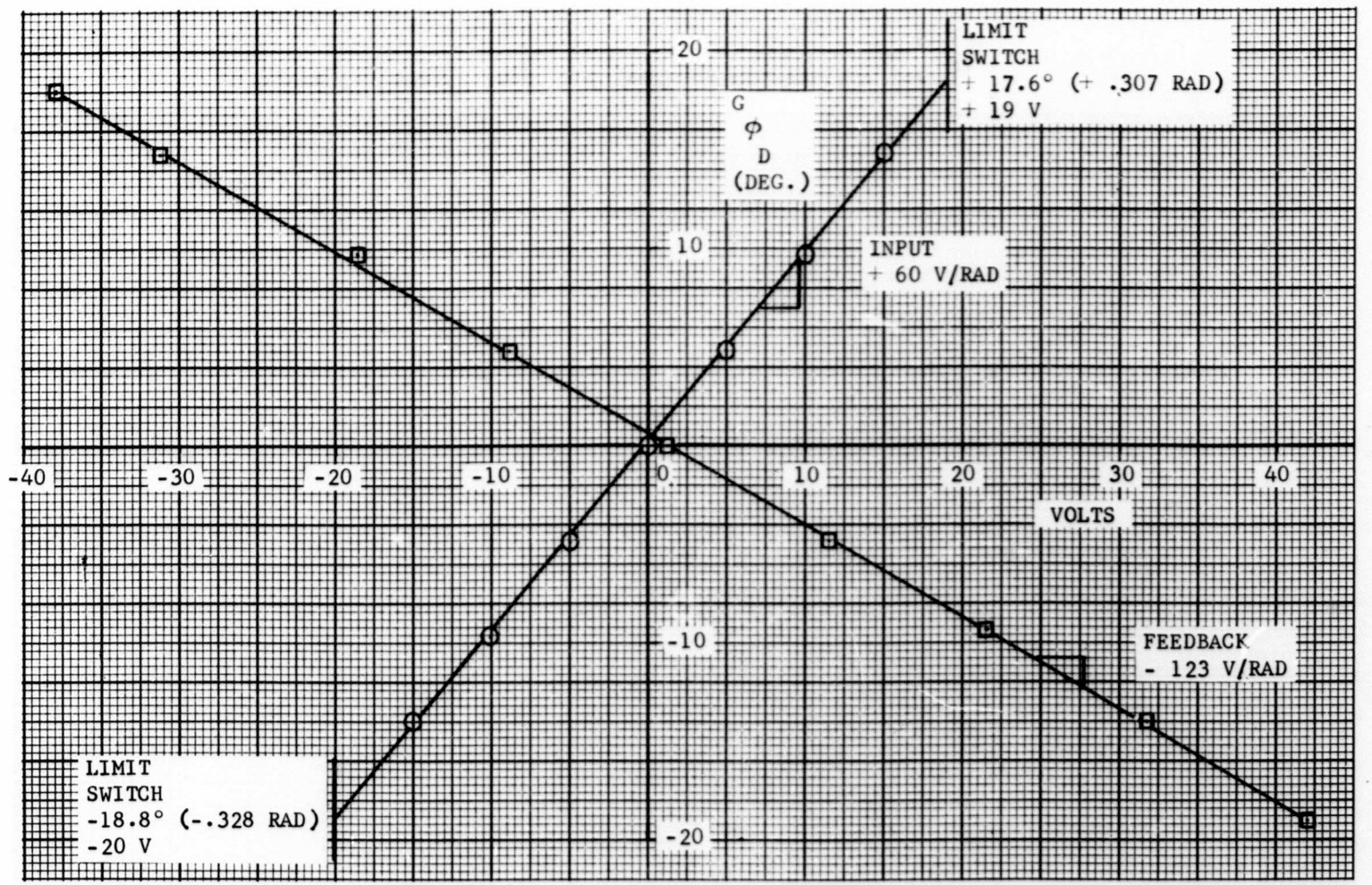

Figure 8. Static Input and Feedback Calibration for G_{ϕ_D}

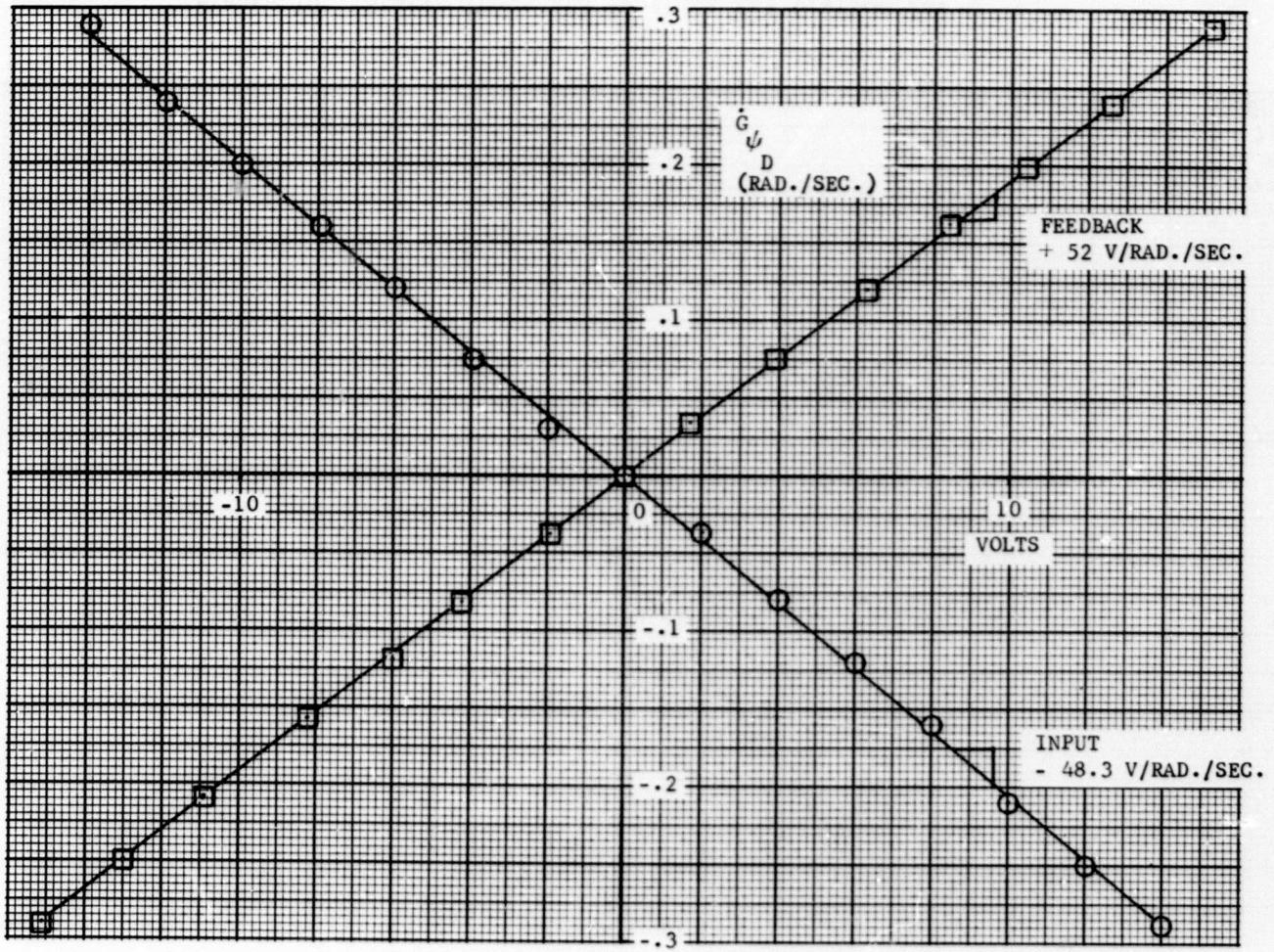

Figure 9. Static Input and Feedback Calibration for $\dot{G}_{\psi_D}$

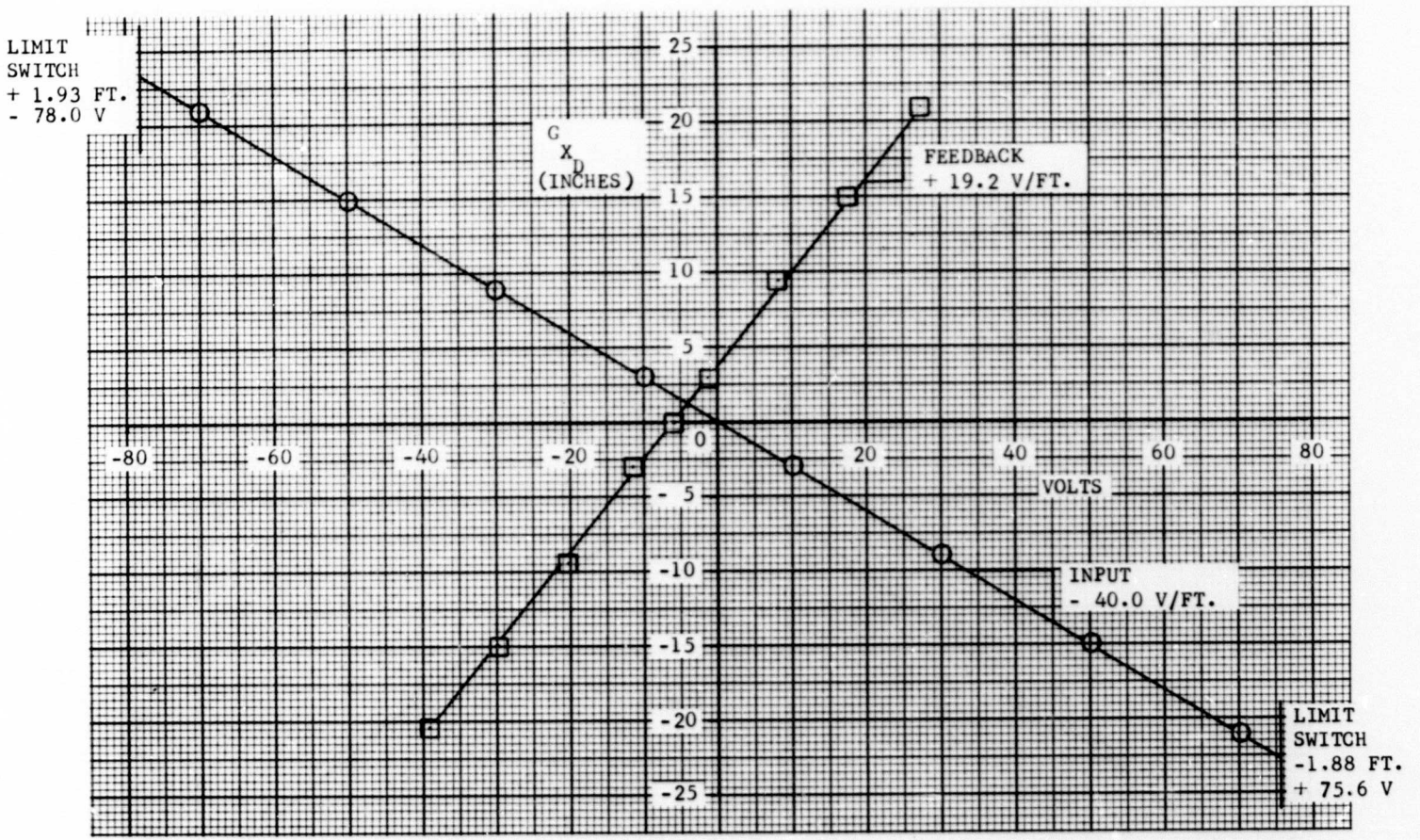

Figure 10. Static Input and Feedback Calibration for G_{X_D}.

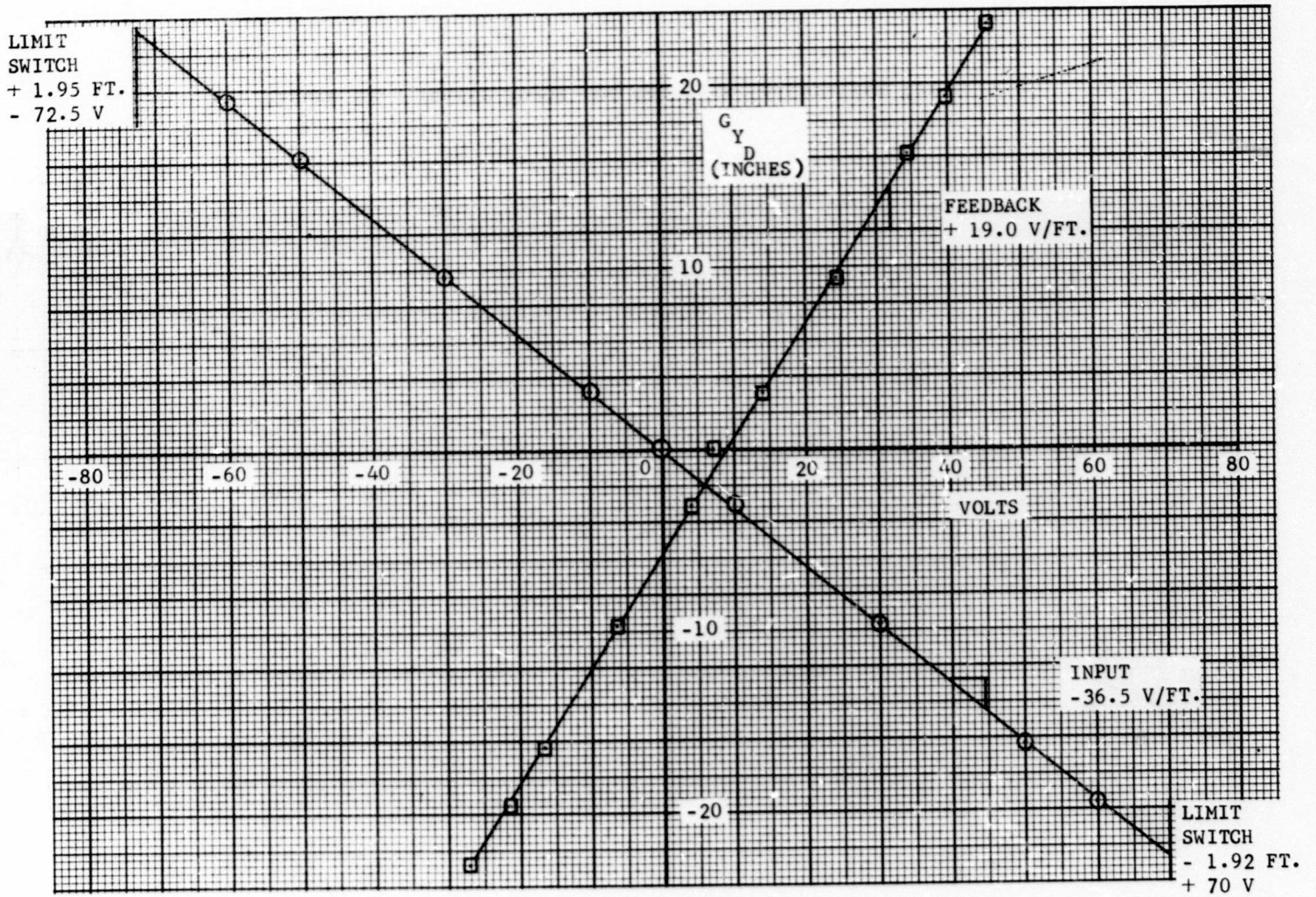

Figure 11. Static Input and Feedback Calibration for G_{Y_D}.

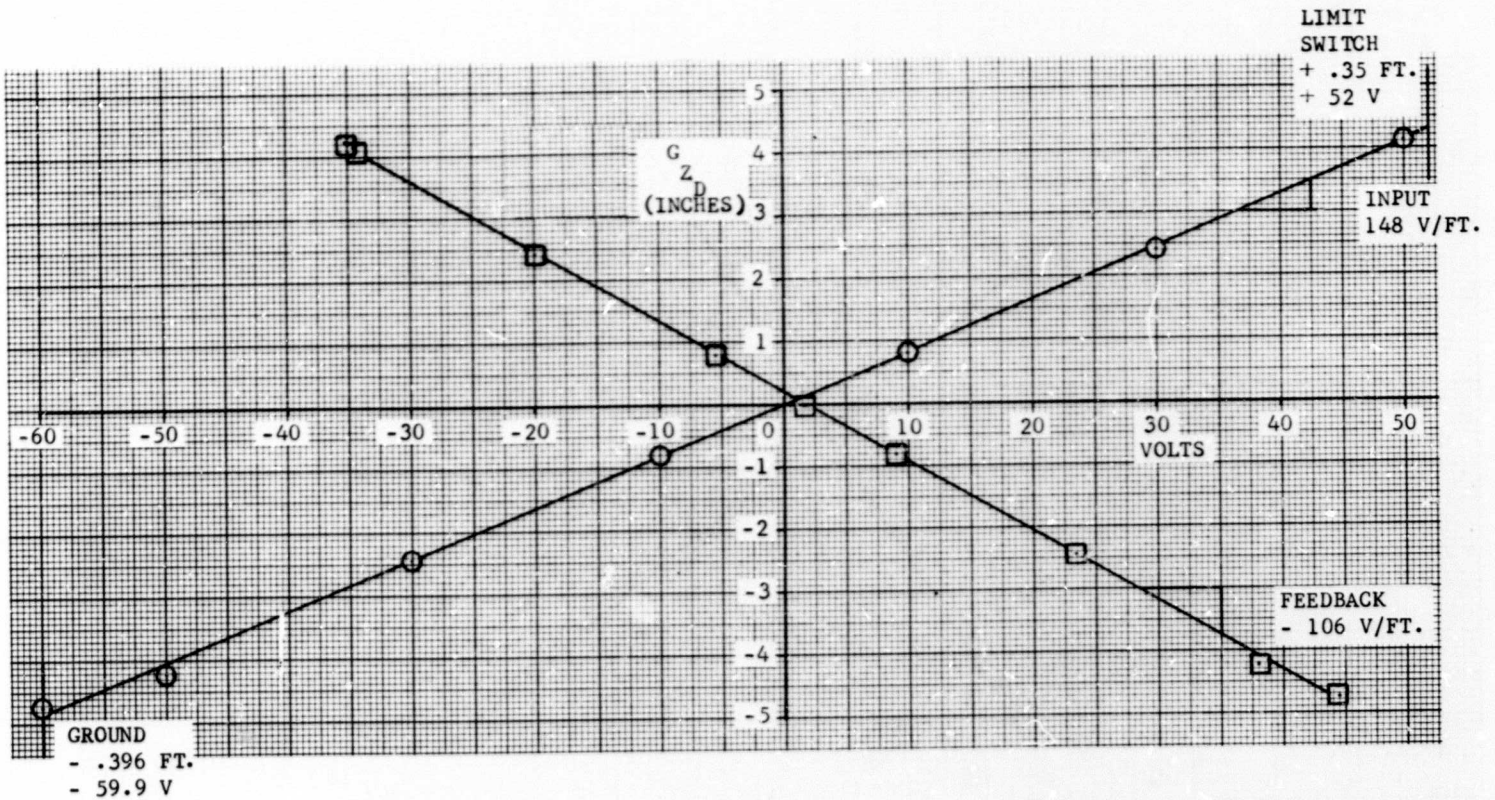

Figure 12. Static Input and Feedback Calibration for G_{Z_D}.

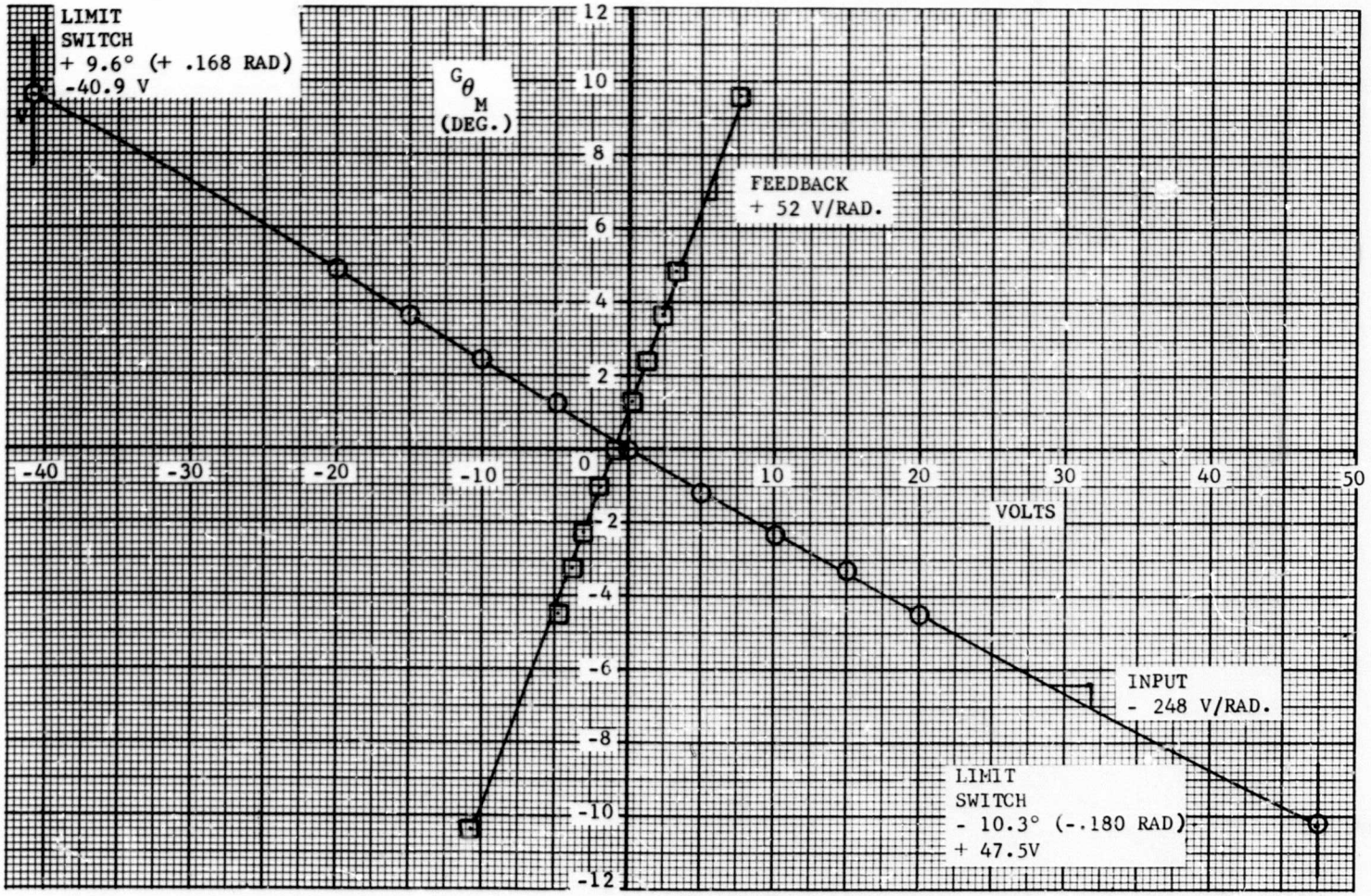

Figure 13. Static Input and Feedback Calibration for G_{θ_M}

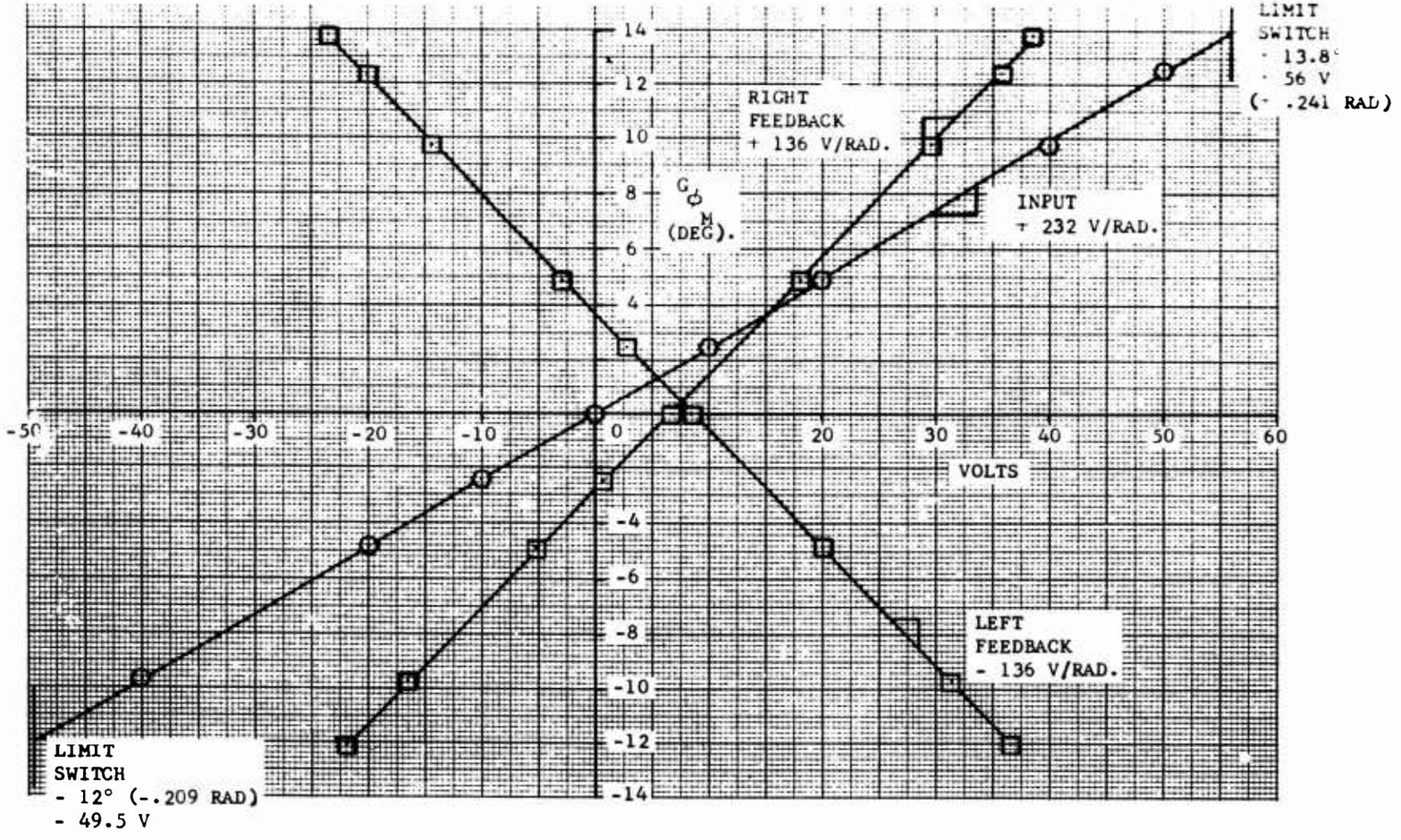

Figure 14. Static Input and Feedback Calibration for G_{ϕ_D}

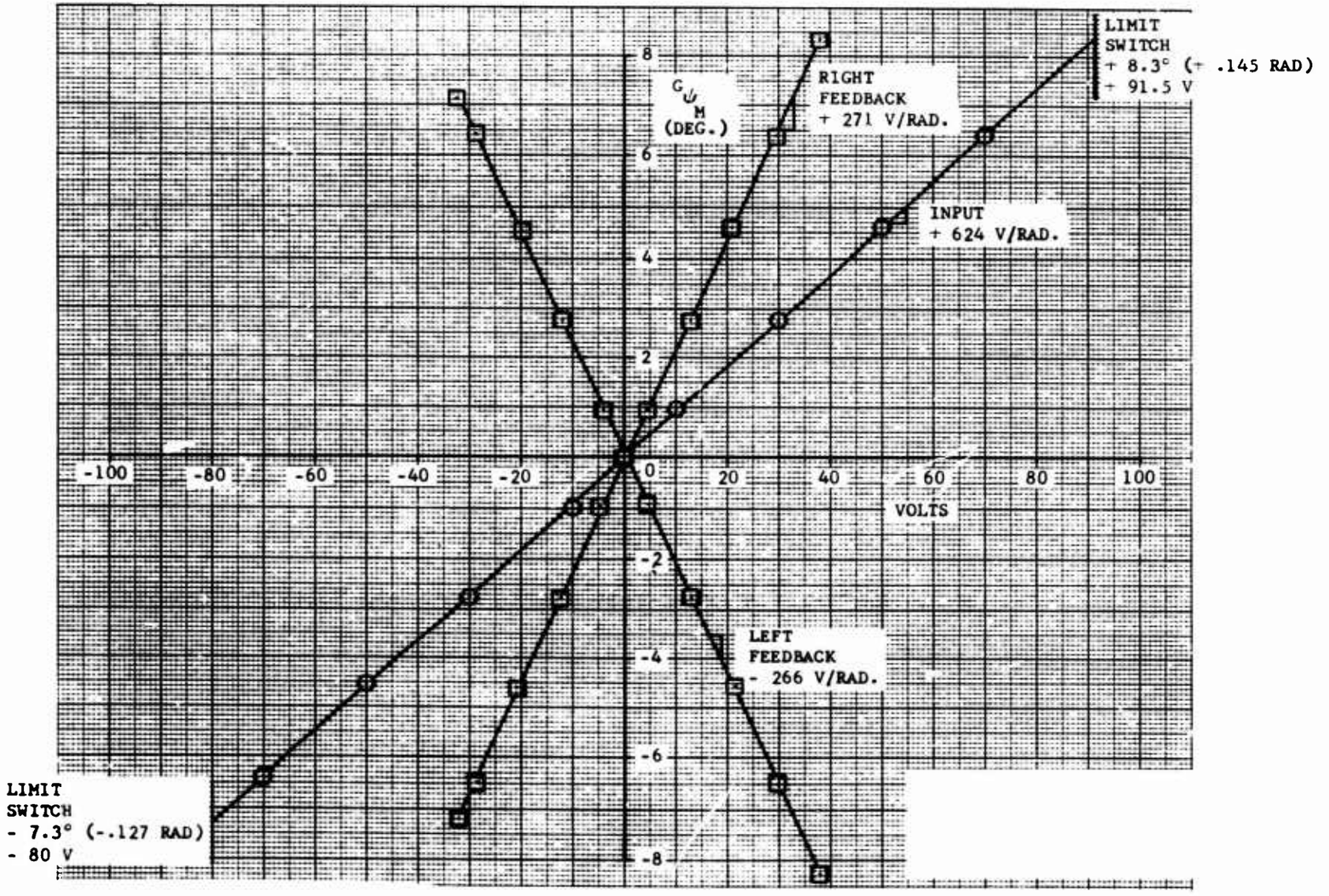

Figure 15. Static Input and Feedback Calibration for G_{ψ_M}

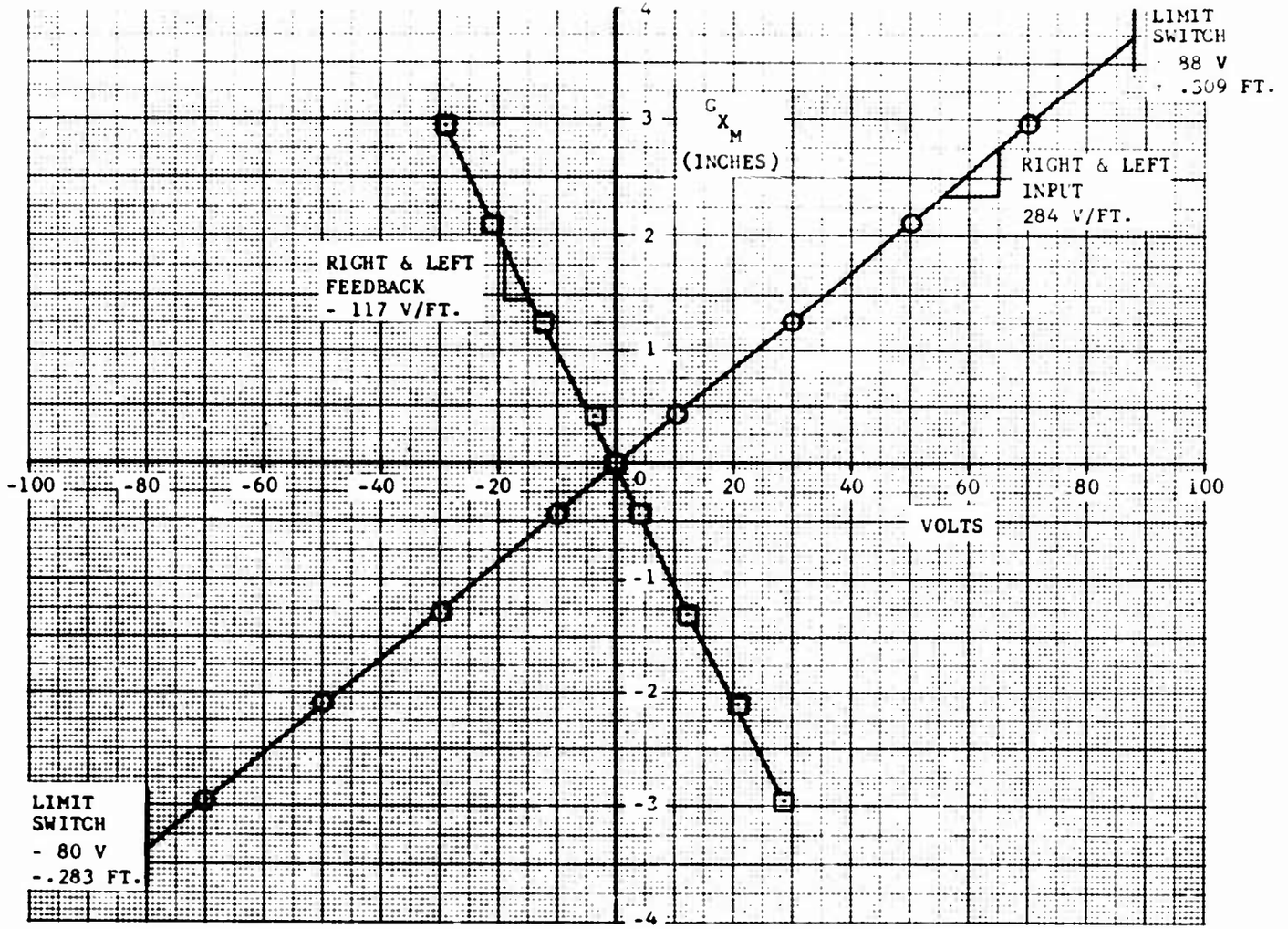

Figure 16. Static Input and Feedback Calibration for G_{X_M}

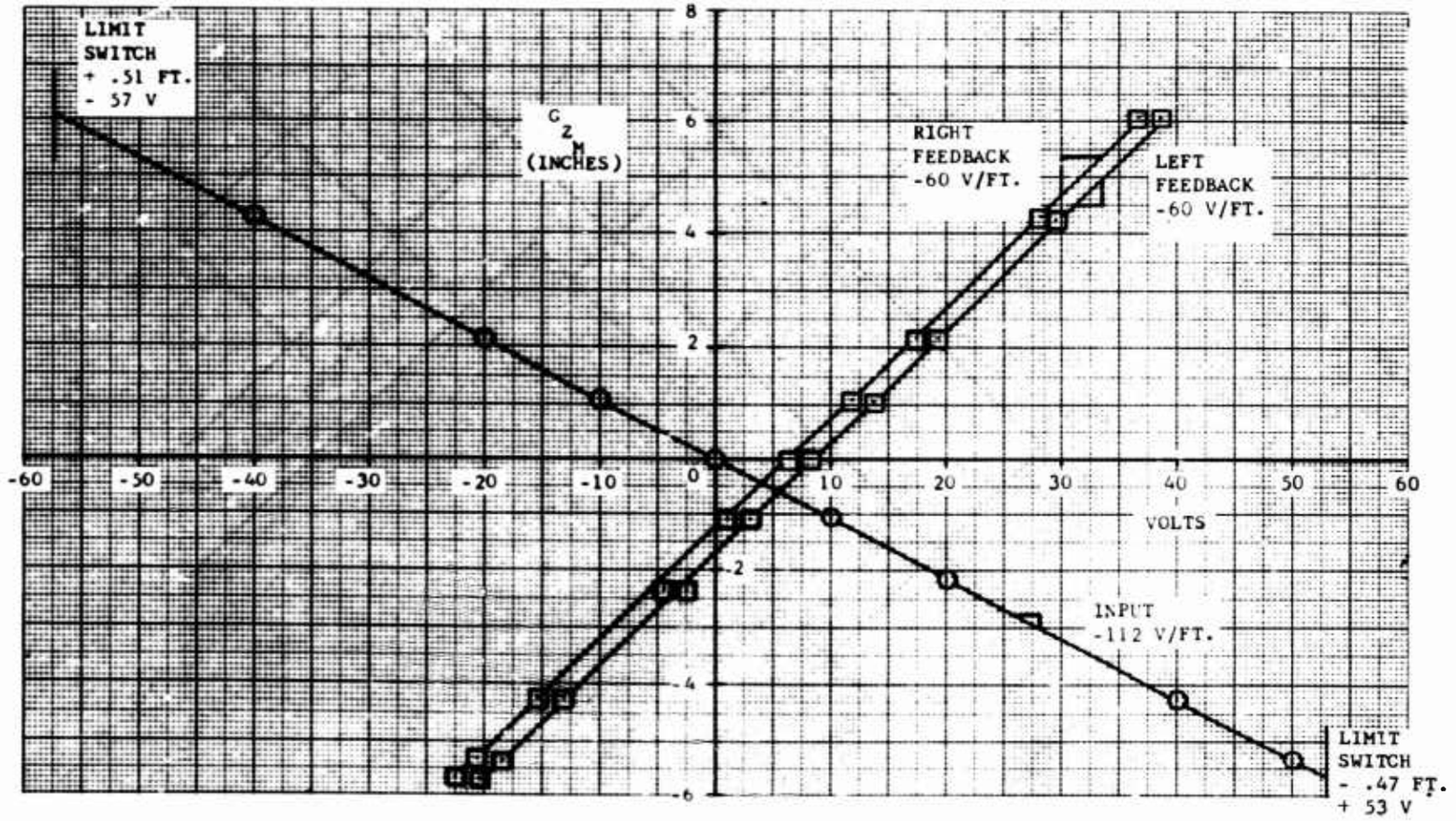

Figure 17. Static Input and Feedback Calibration for G_{Z_M}

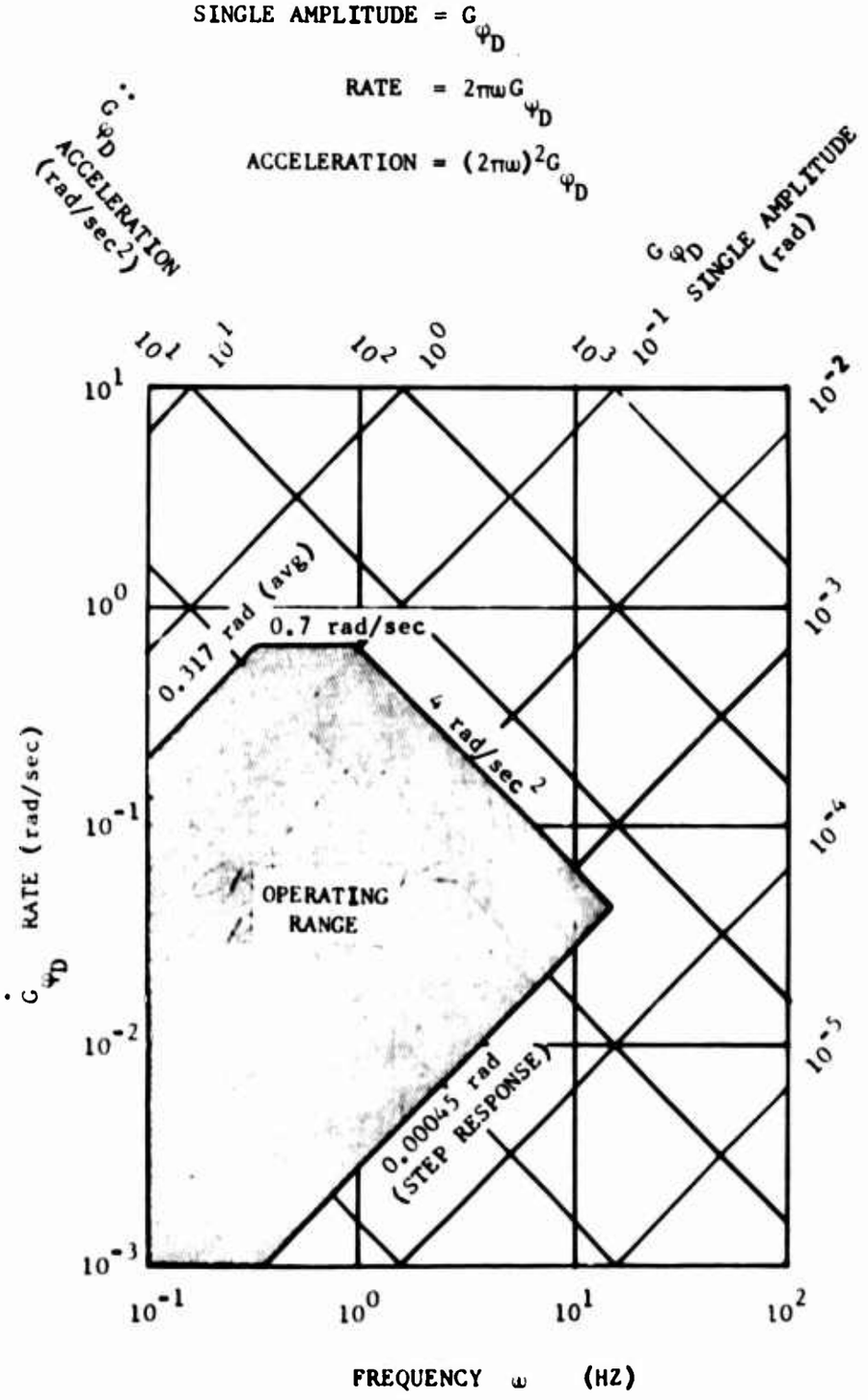

Figure 18. Performance Envelope for the Visual Display Roll Axis, G_{φ_D}.

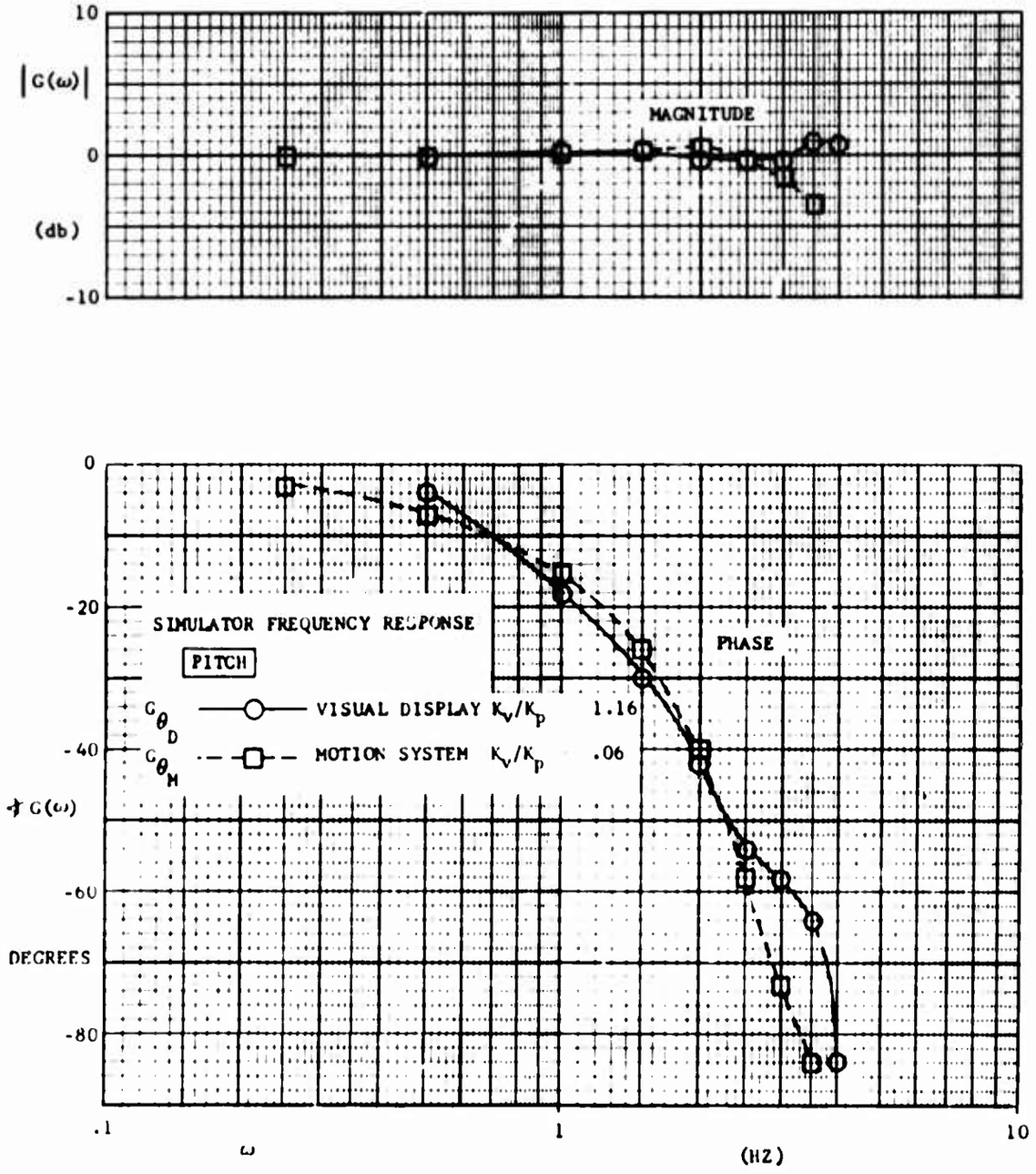

Figure 19. Frequency Response for G_{θ_D} and G_{θ_M}

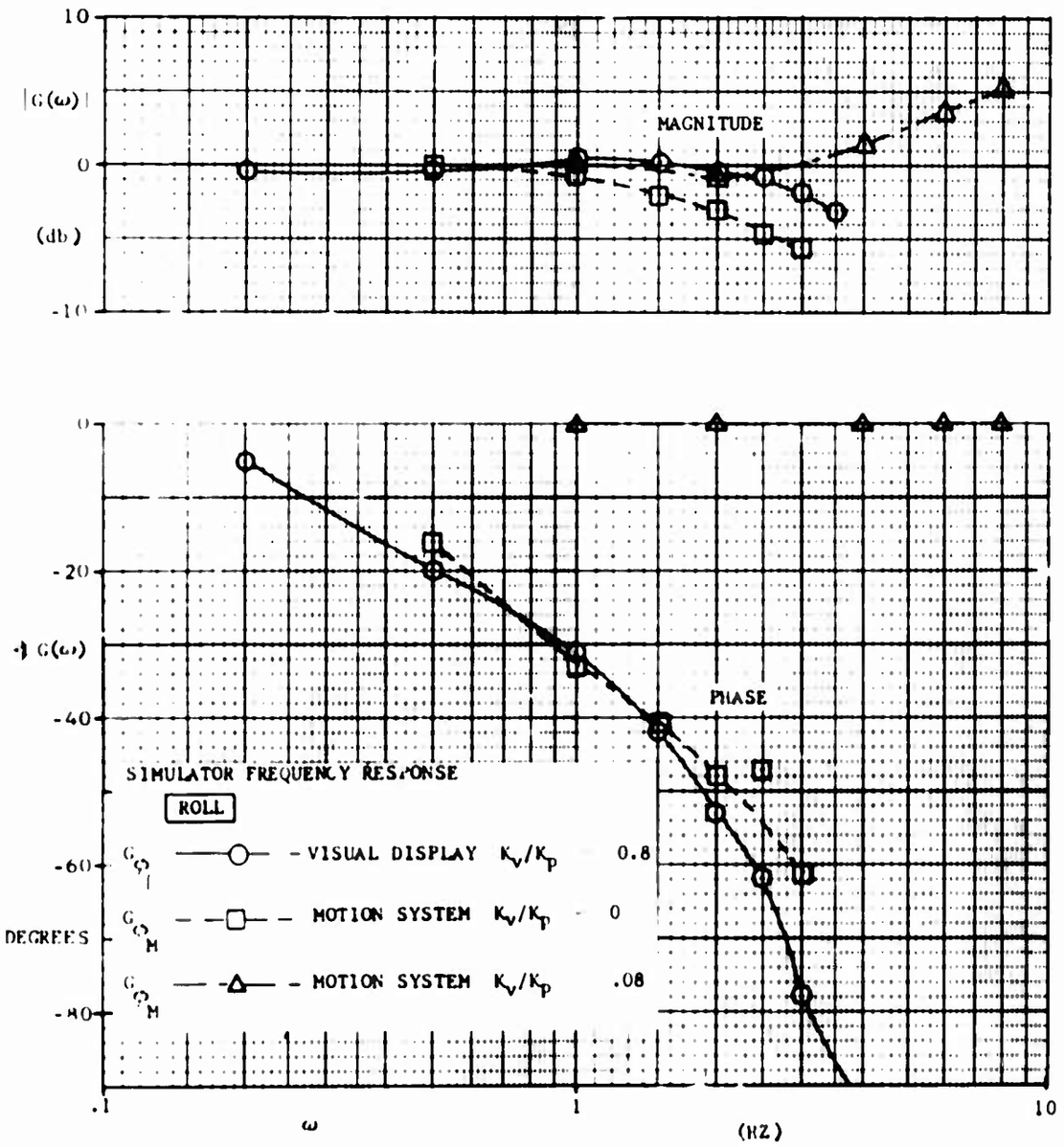

Figure 20. Frequency Response for G_{φ_D} and G_{φ_M}

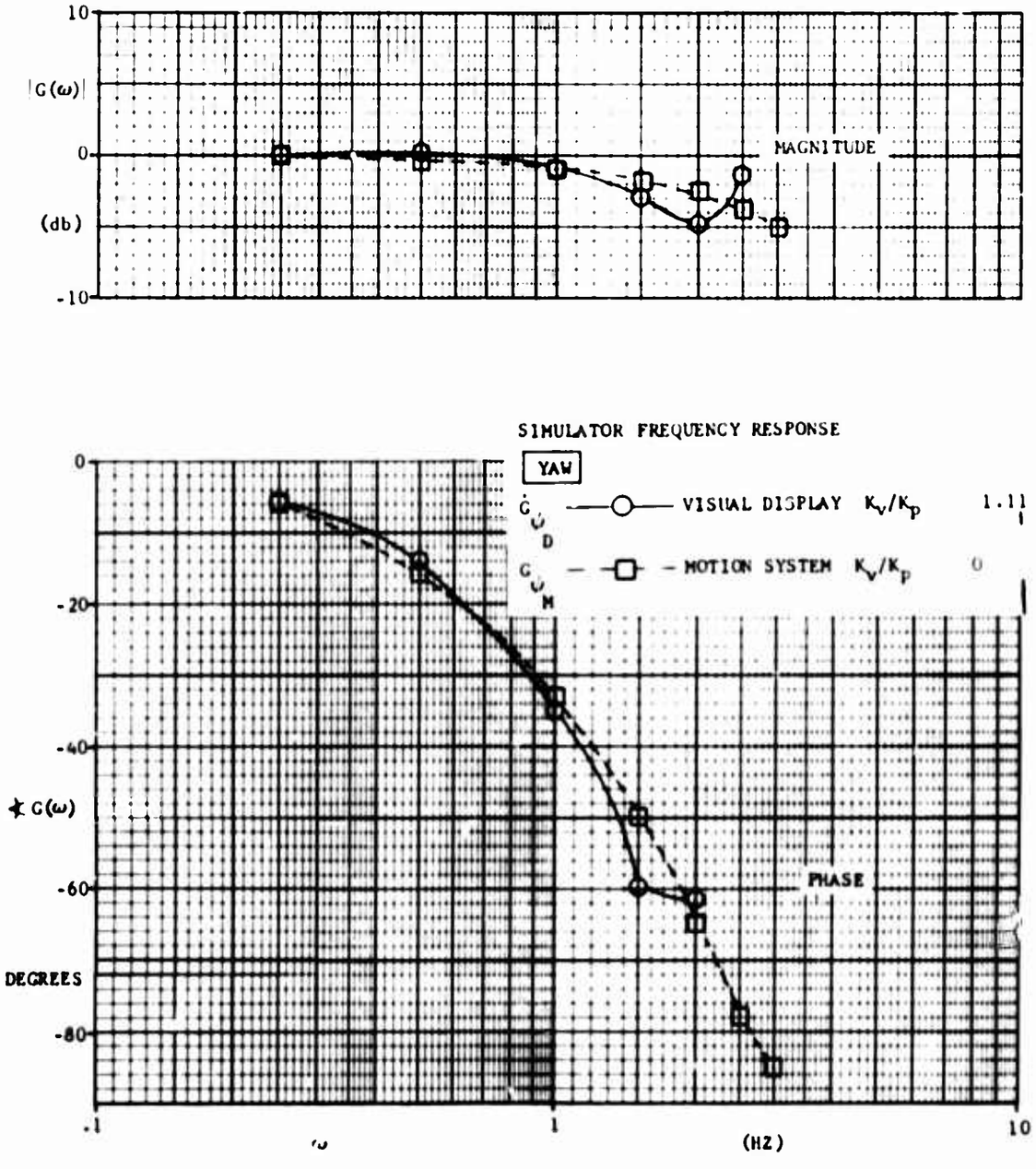

Figure 21. Frequency Response for $\dot{G}_{\psi_D}$ and G_{ψ_M}

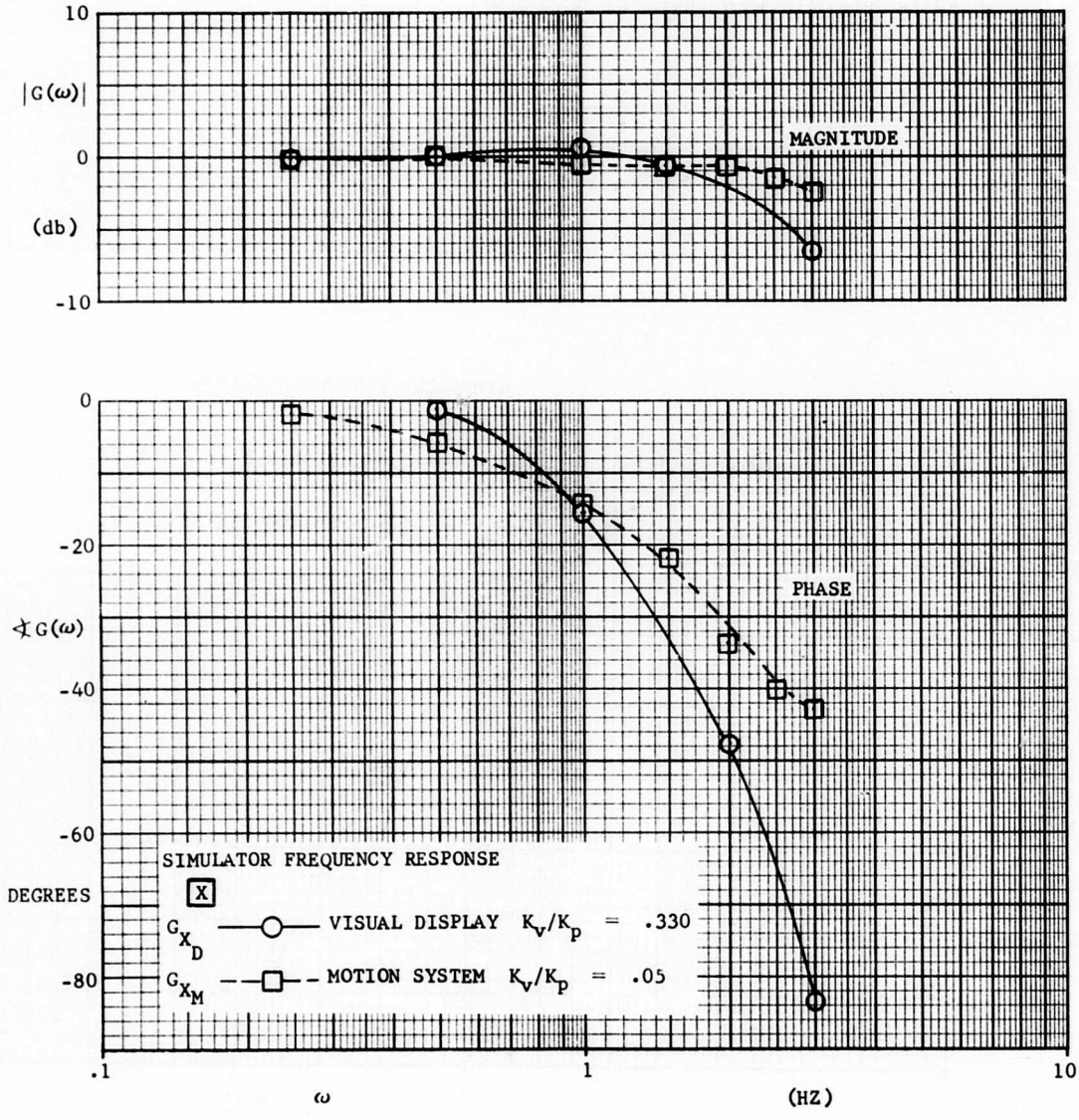

Figure 22. Frequency Response for G_{X_D} and G_{X_M}.

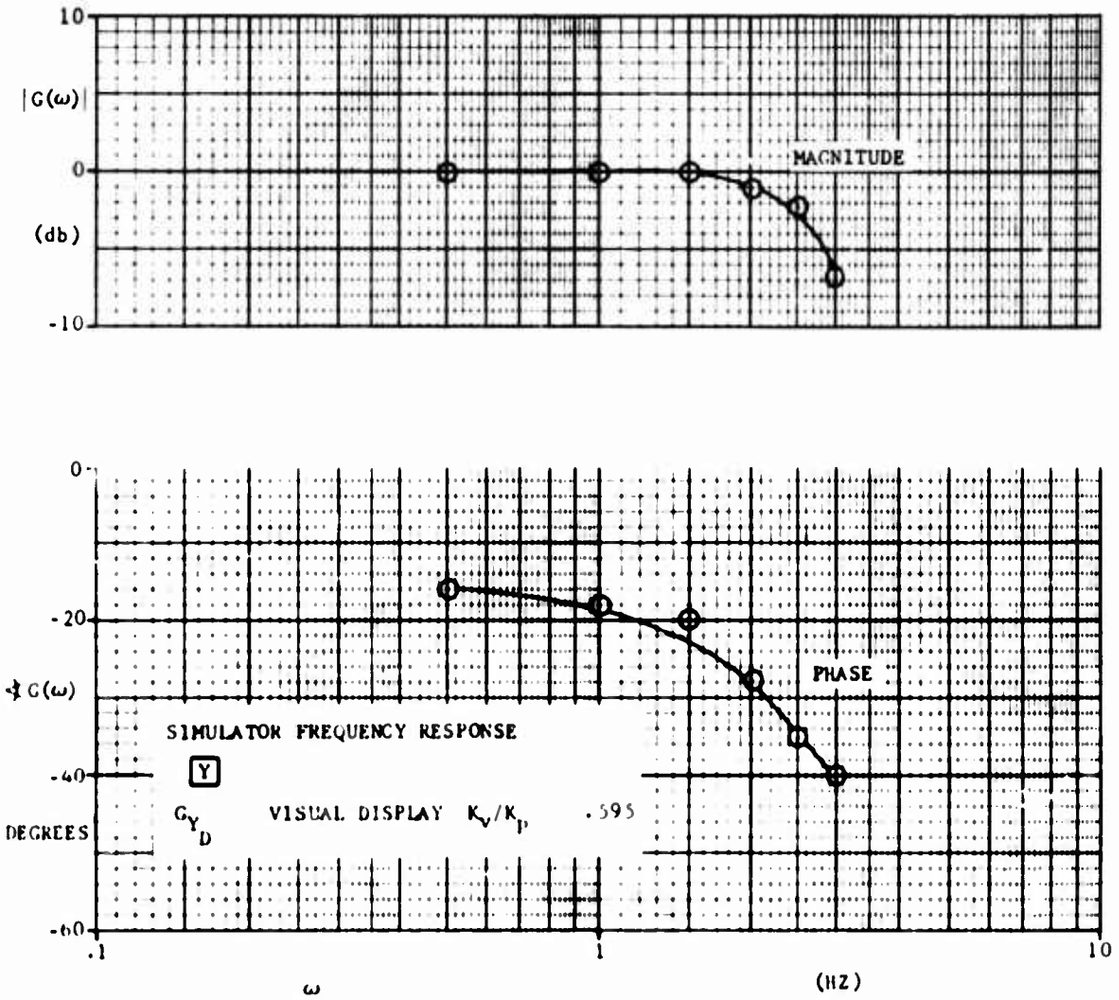

Figure 23. Frequency Response for G_{Y_D}.

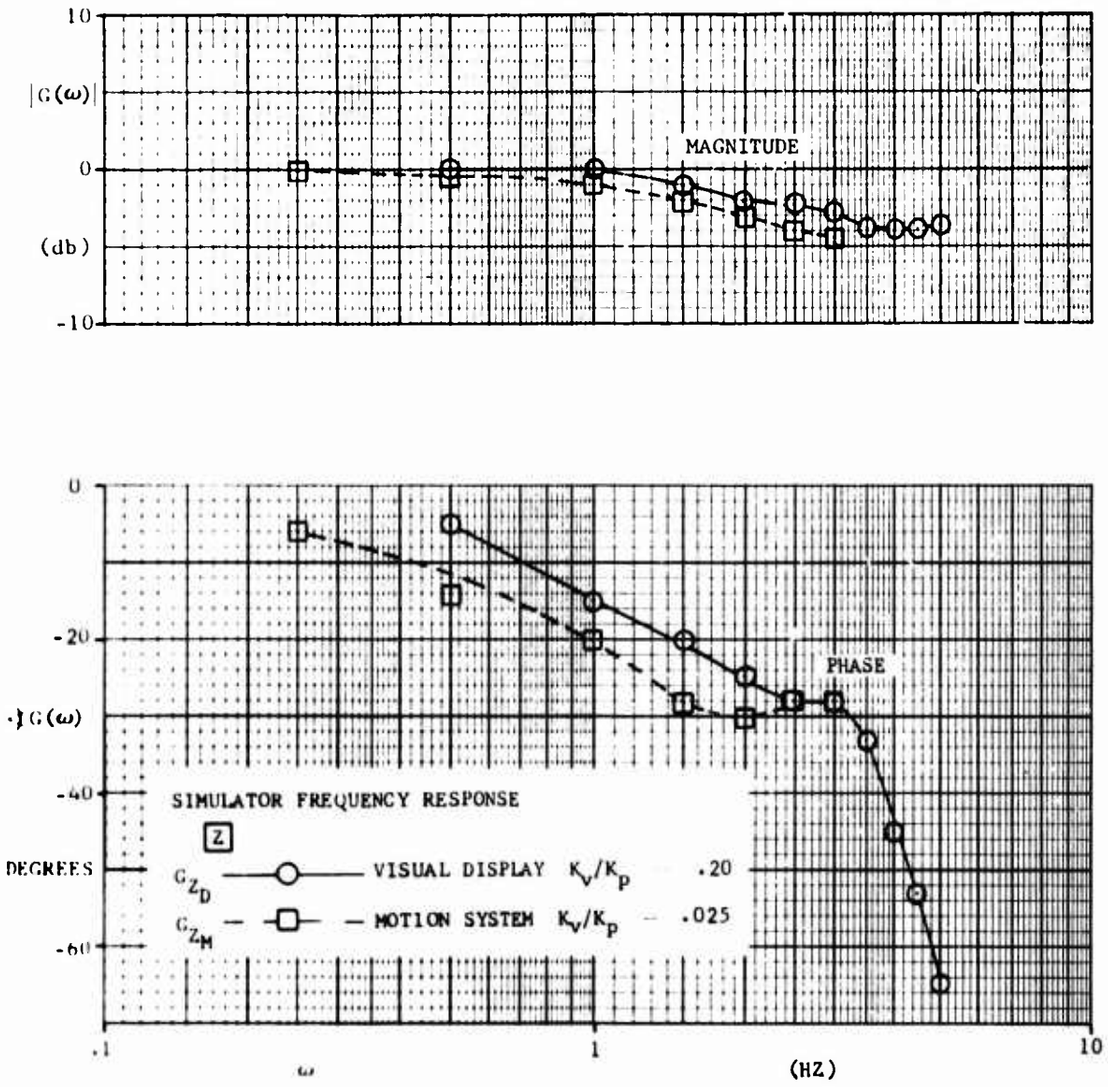

Figure 24. Frequency Response for G_{Z_D} and G_{Z_M}

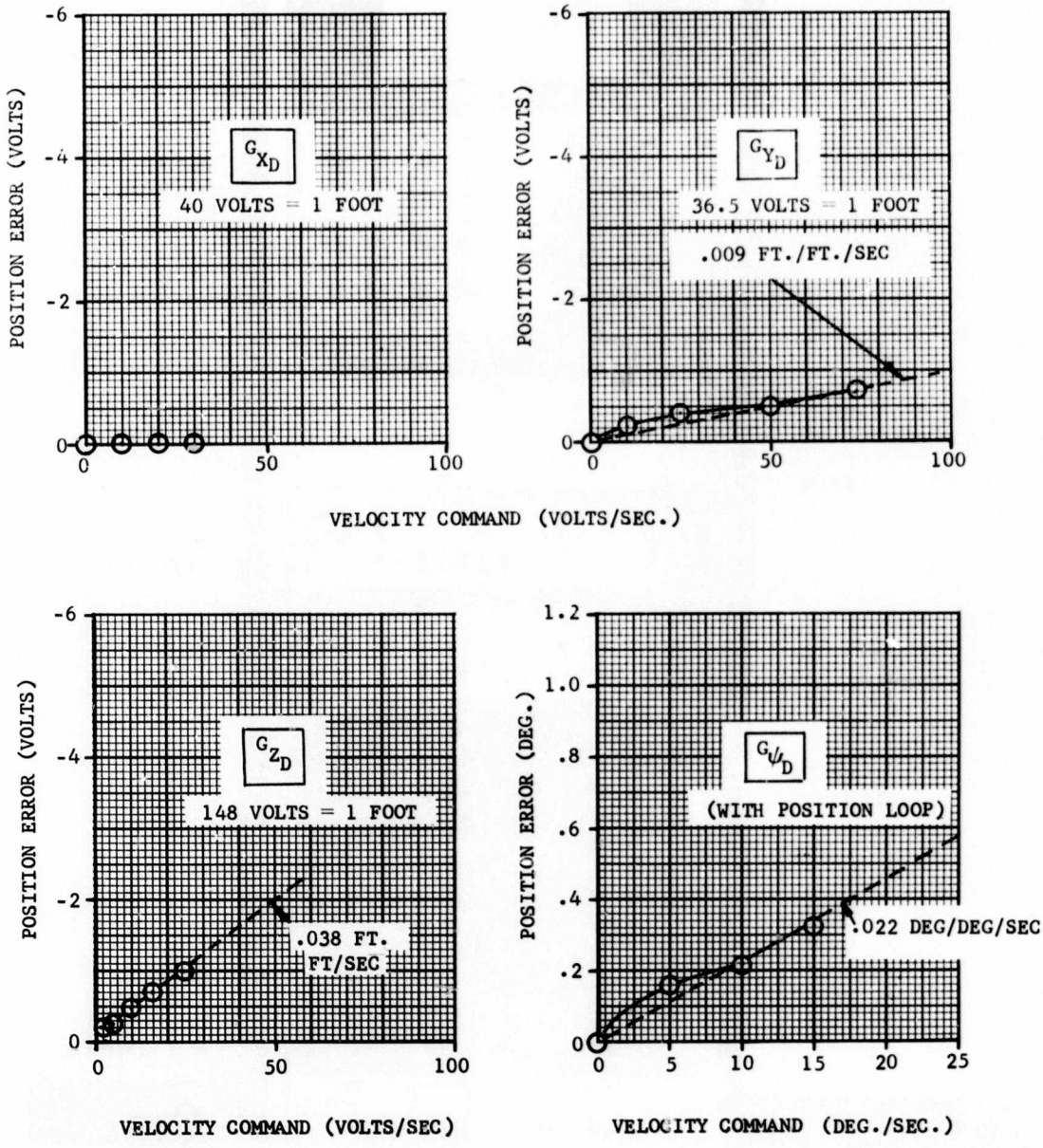

Figure 25. Velocity Error for the Visual Display.

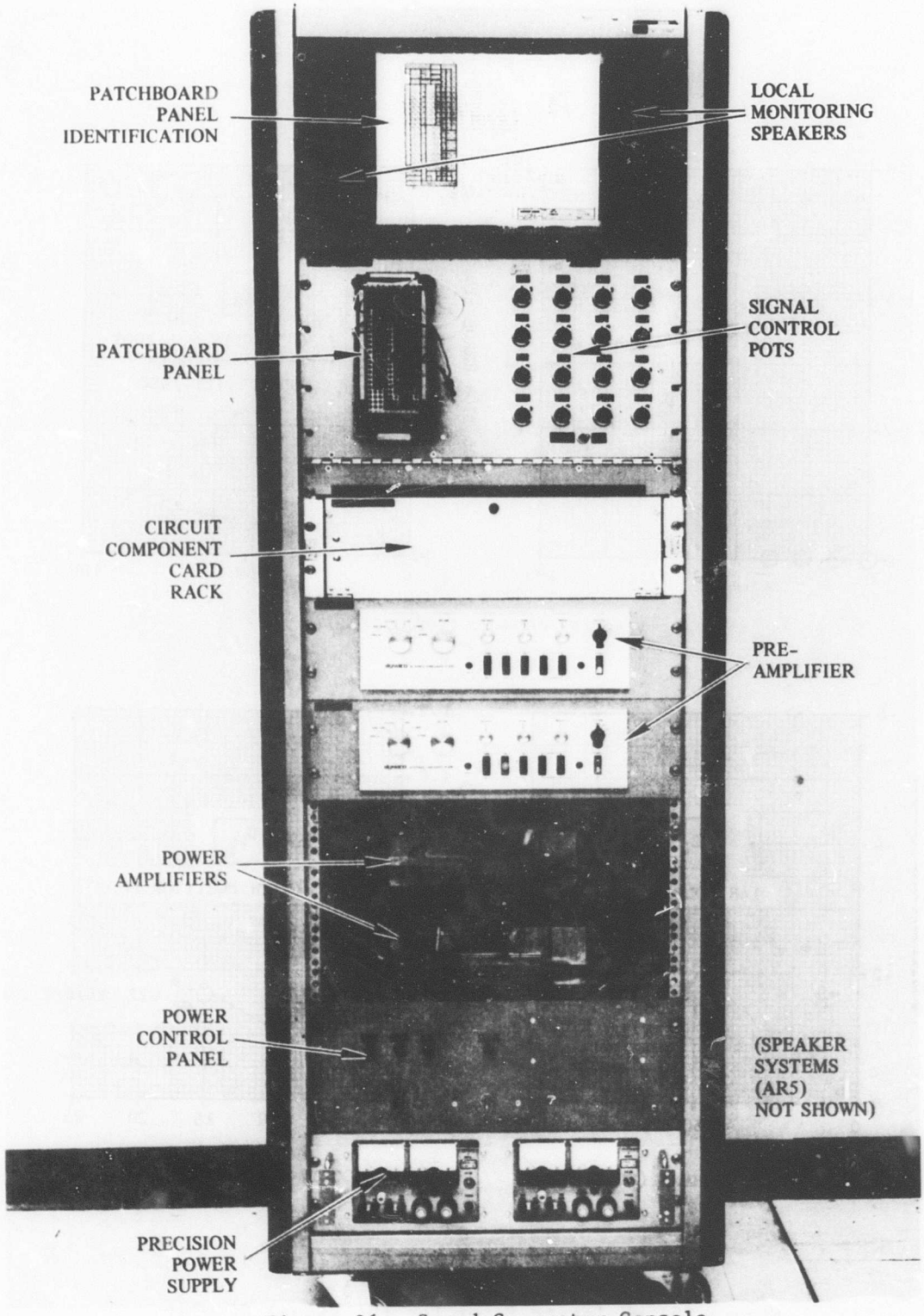

Figure 26. Sound Generator Console.

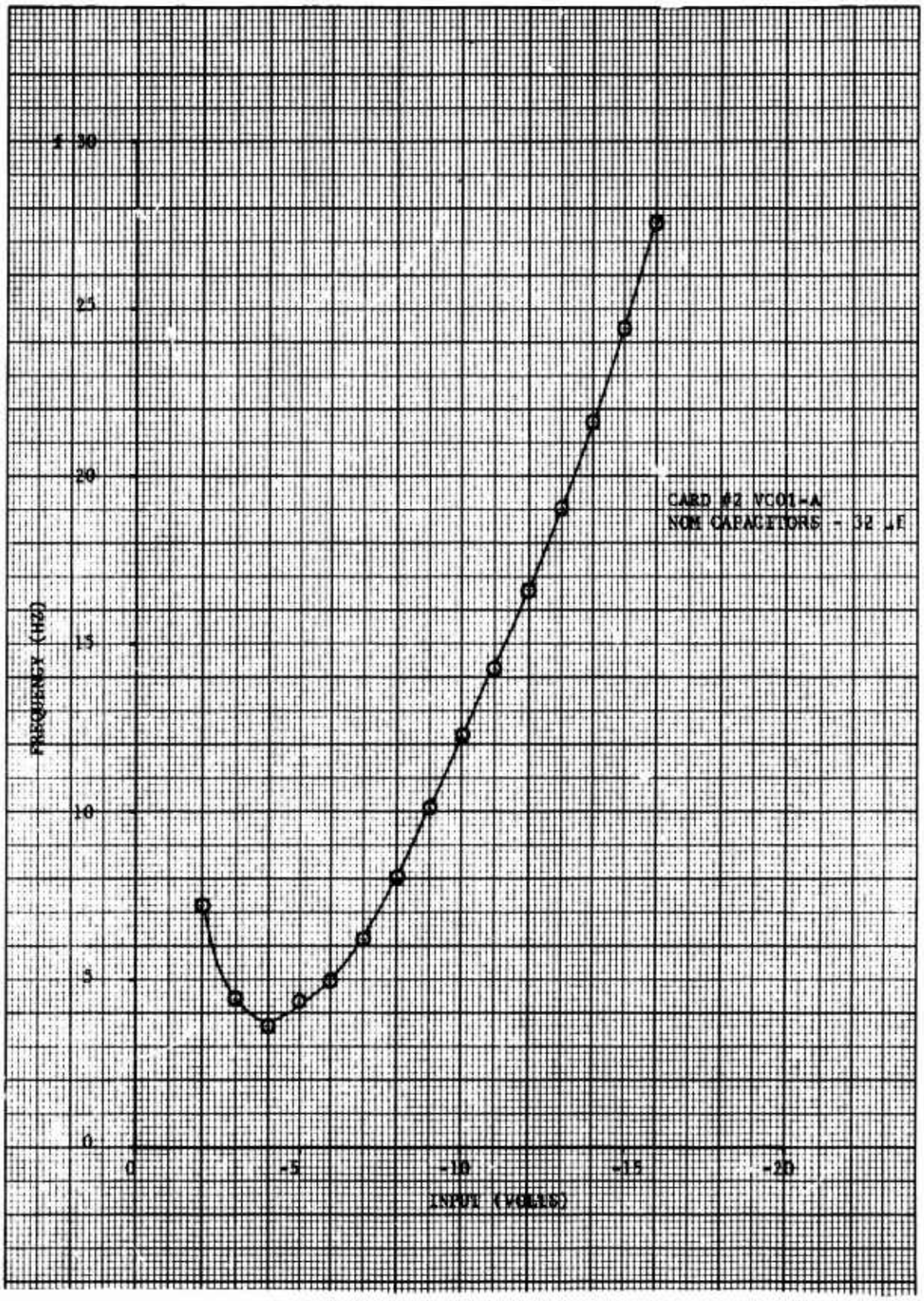

Figure 27. Sound Generator Calibration, 3-30 Hz Range.

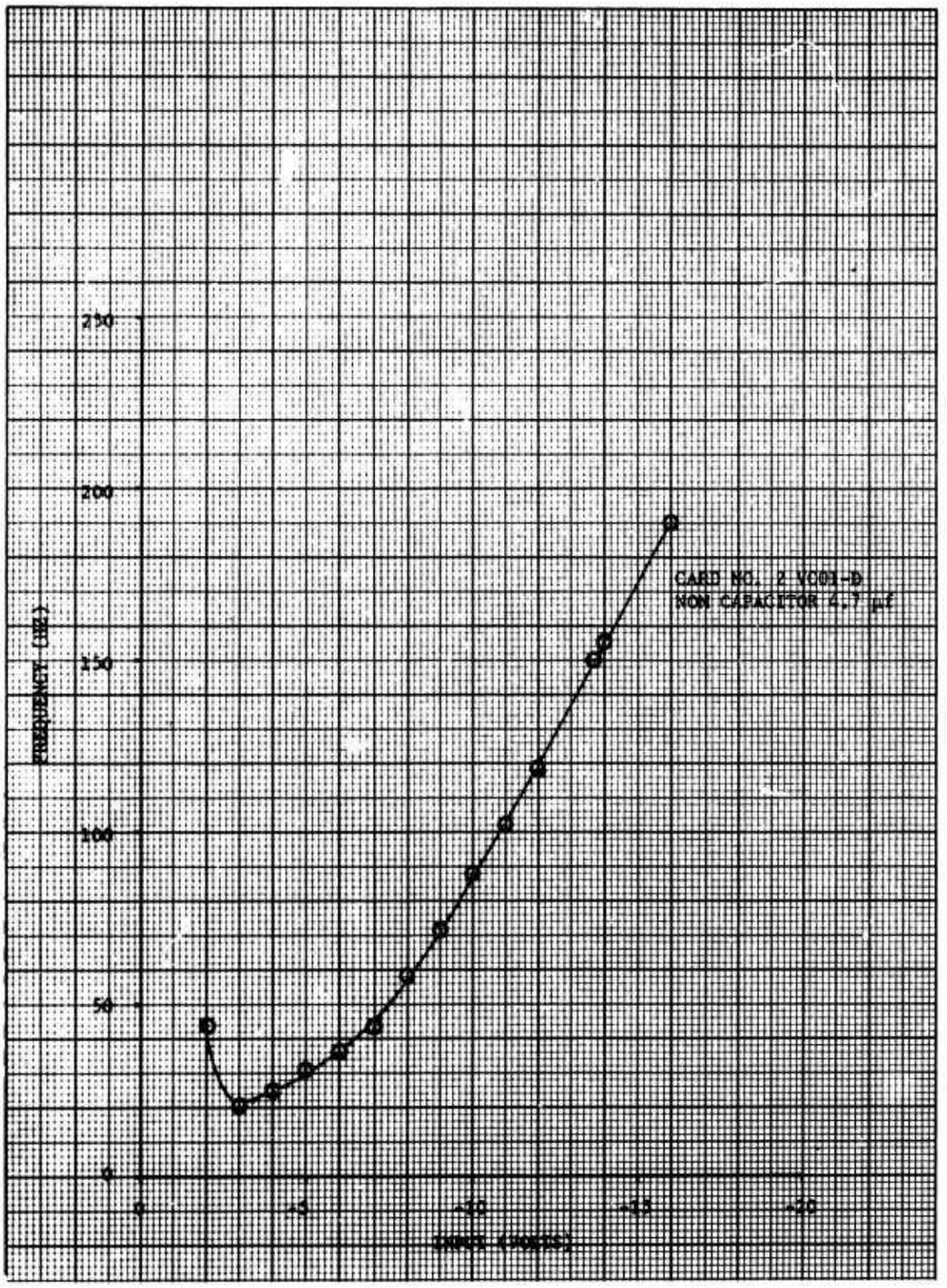

Figure 28. Sound Generator Calibration, 20-200 Hz Range.

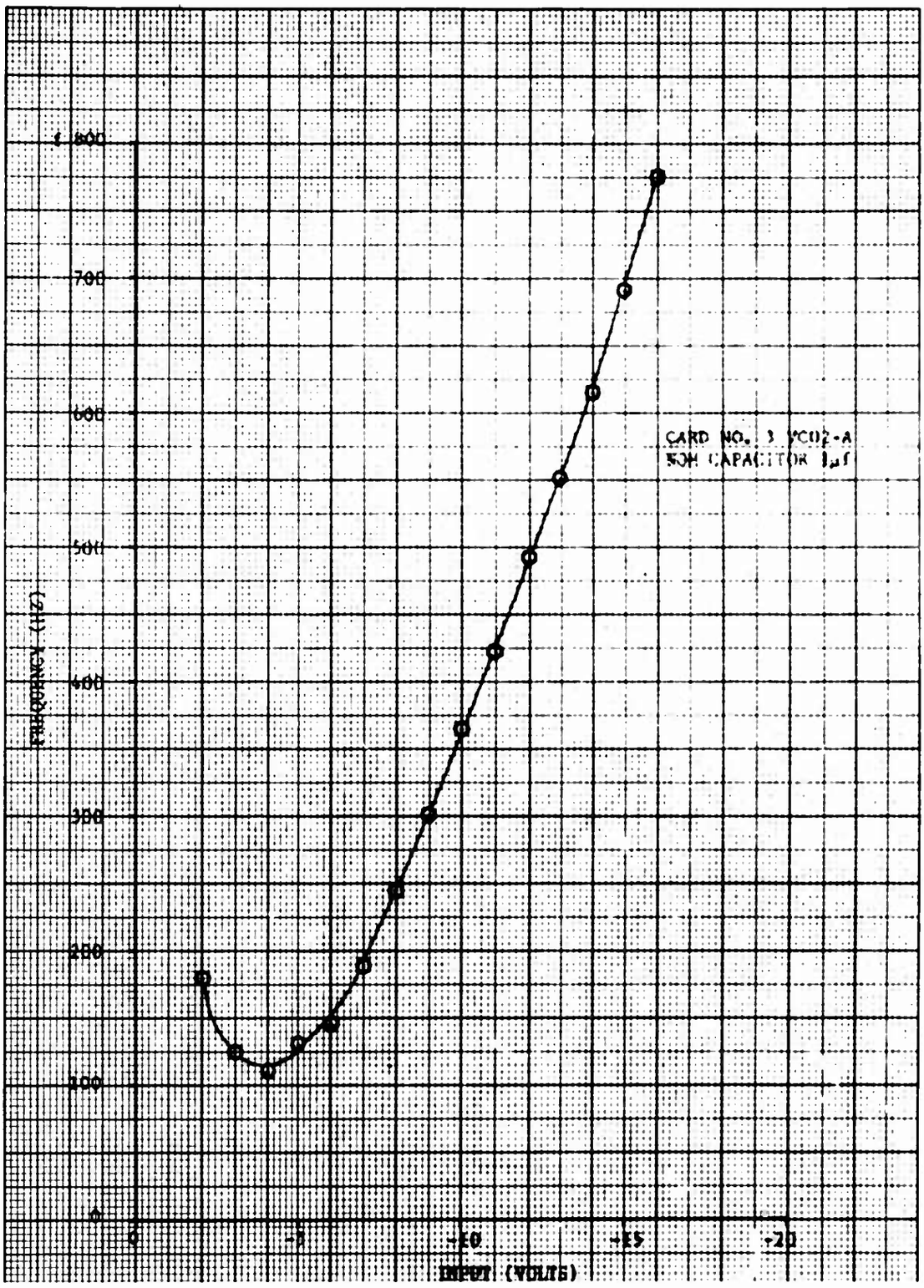

Figure 29. Sound Generator Calibration, 100-800 Hz Range.

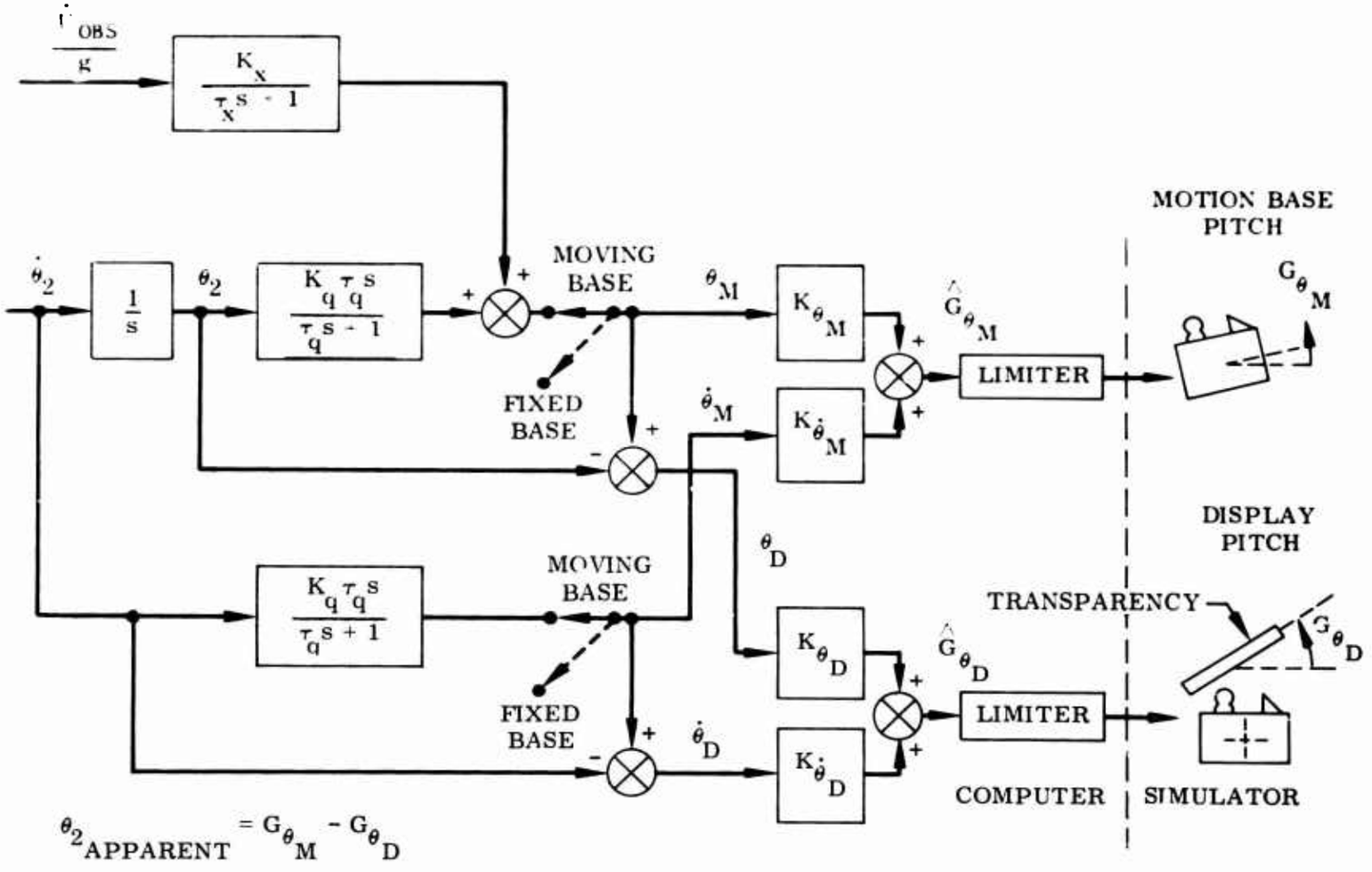

Figure 30. Mechanization A, Longitudinal Motion System - Visual Display Interface.

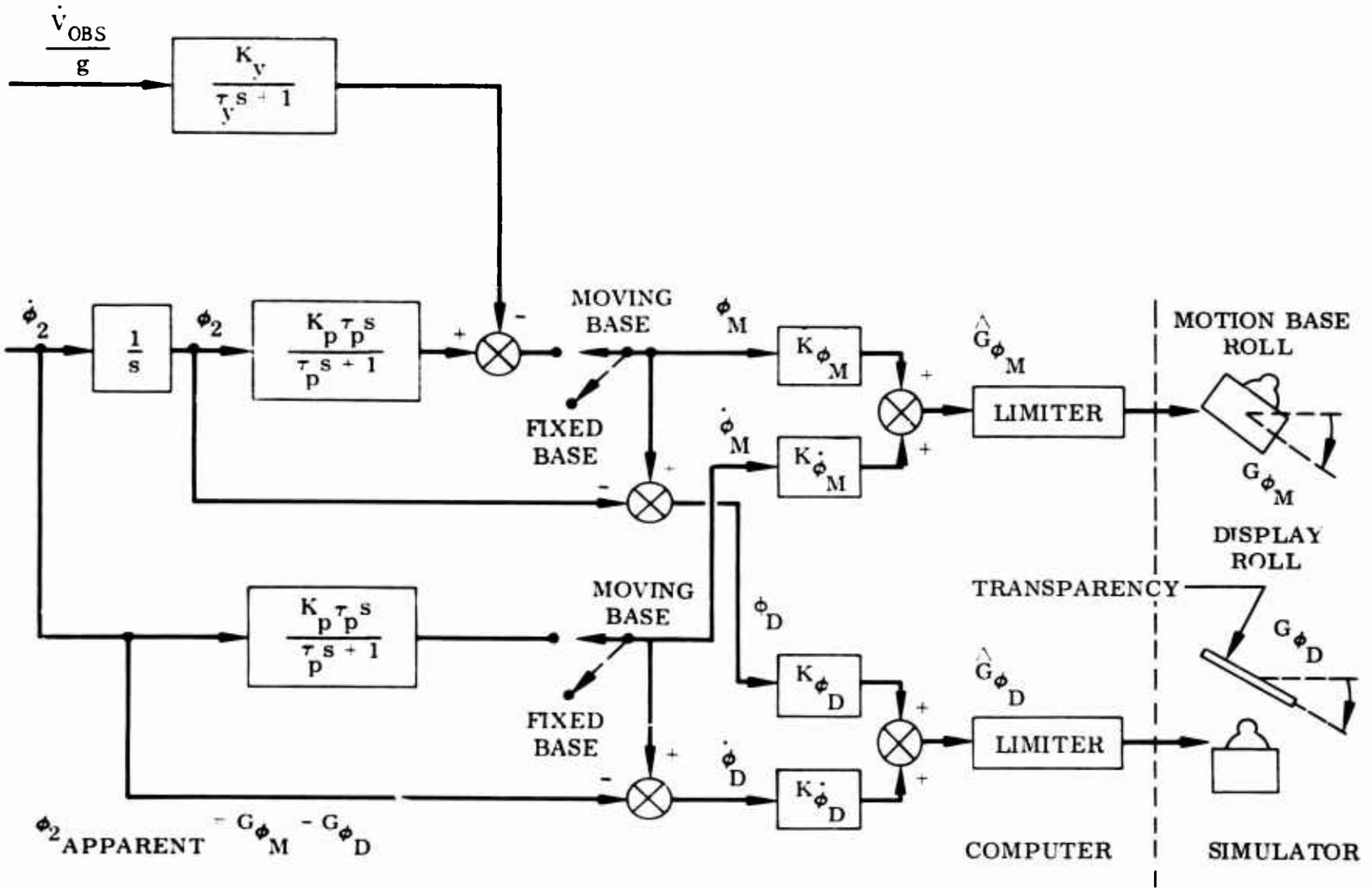

Figure 31. Mechanization A, Lateral Motion System - Visual Display Interface.

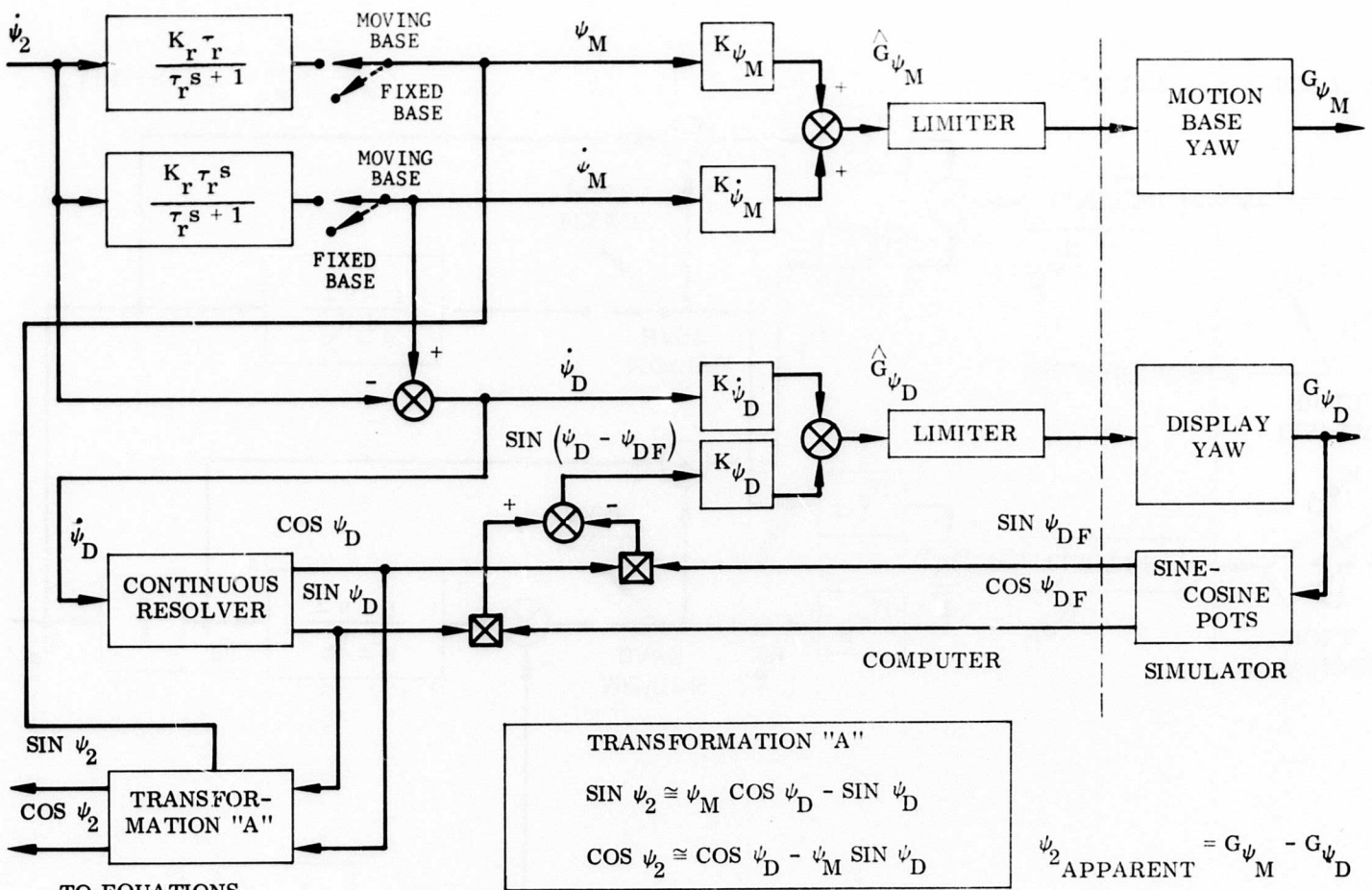

Figure 32. Mechanization A, Yaw Motion System - Visual Display Interface.

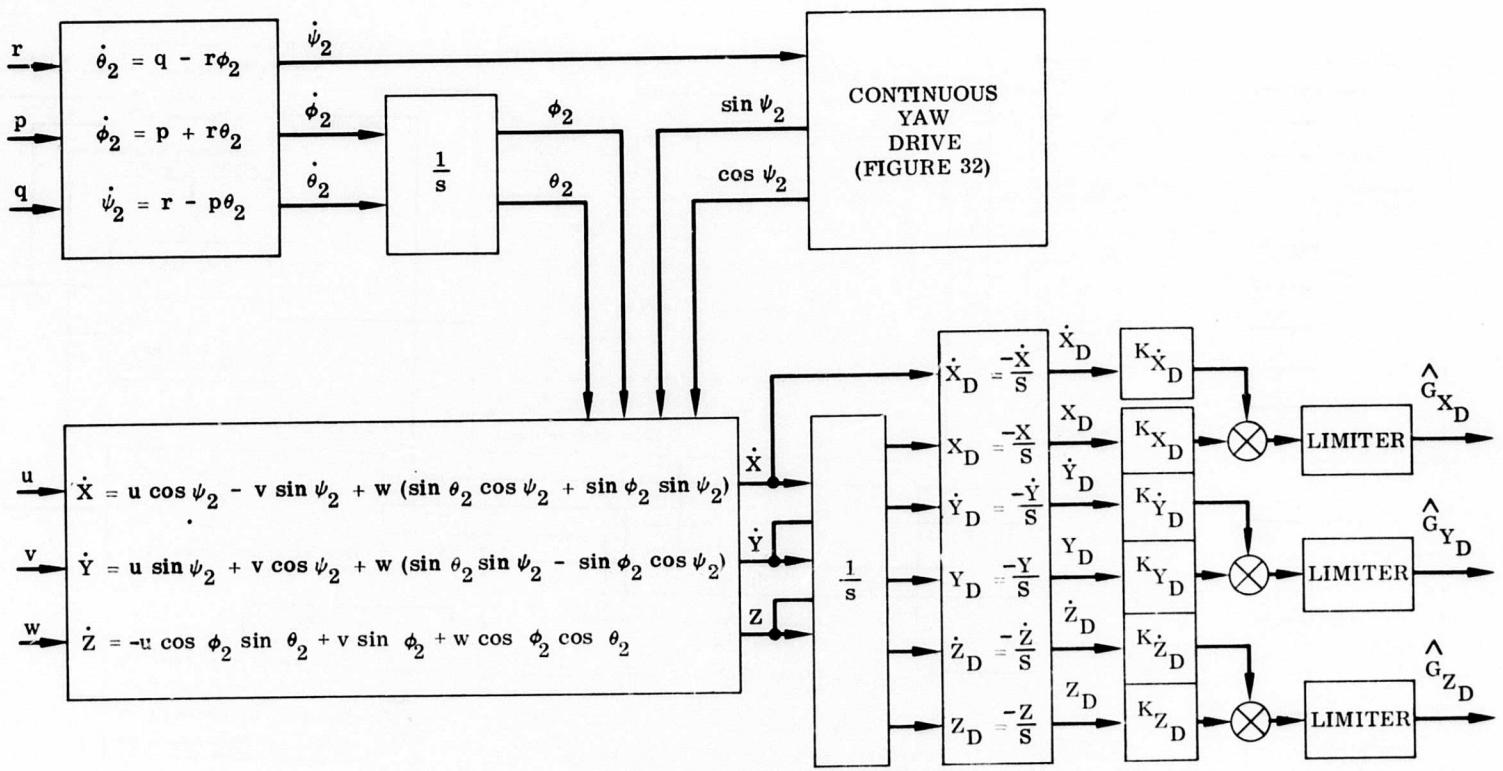

Figure 33. Mechanization A, Visual Display Linear Actuator Interface.

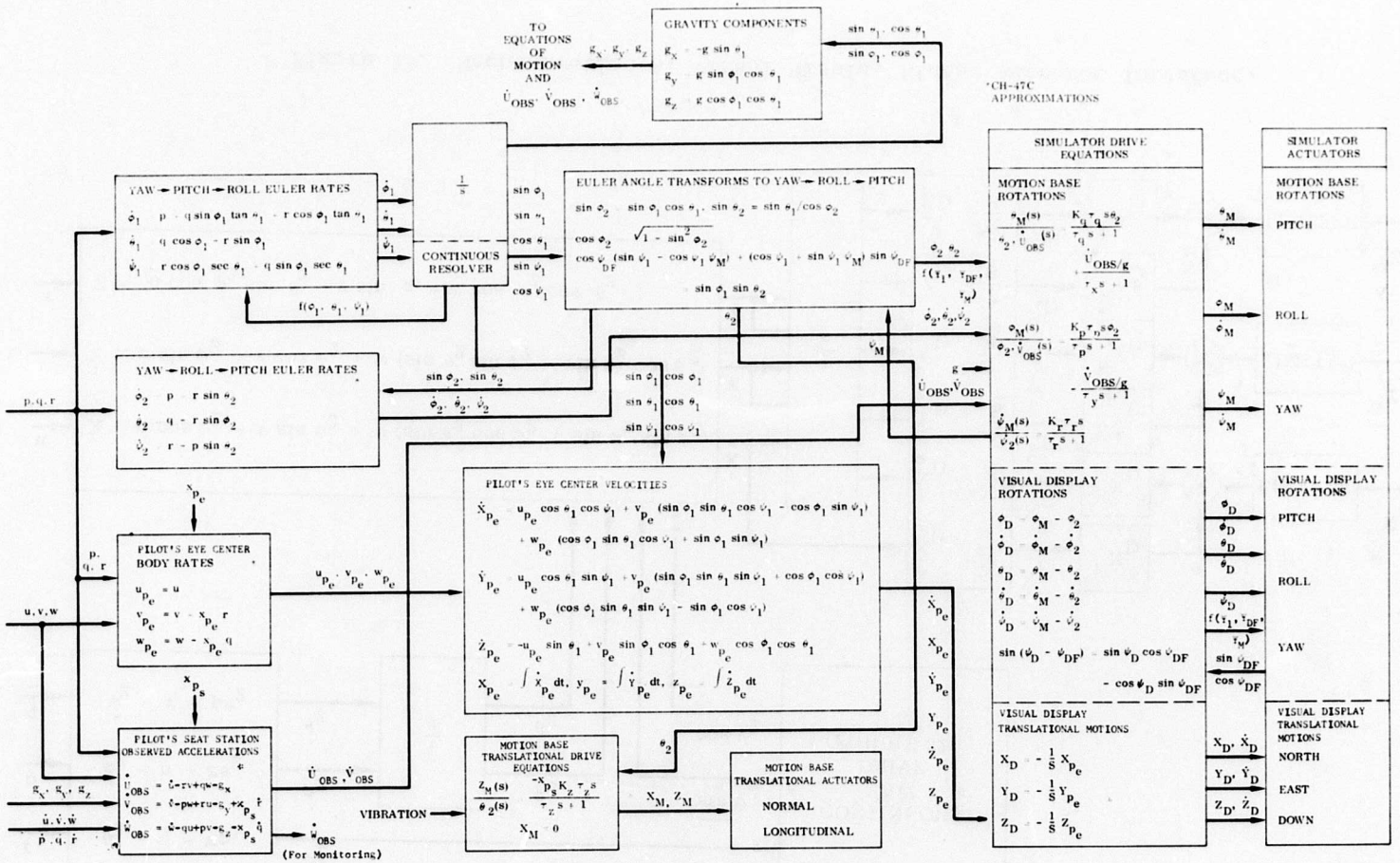

Figure 34. Mechanization B, General Block Diagram.

$\sin(\Psi_1-\Psi_2) = \sin\varphi_1\sin\theta_2$ $\quad\quad$ $\Psi_2 = \Psi_M - \Psi_D = \Psi_M - \Psi_{DF}$

$\sin(\Psi_1 + \Psi_{DF} - \Psi_M) = \sin\Psi_{DF}(\cos\Psi_1+\sin\Psi_1\Psi_M)+\cos\Psi_{DF}(\sin\Psi_1 - \cos\Psi_1\Psi_M) = \sin\varphi_1\sin\theta_2$

$\Psi_D = \Psi_{DF}$, $\sin\Psi_M=\Psi_M$, $\cos\Psi_M=1$

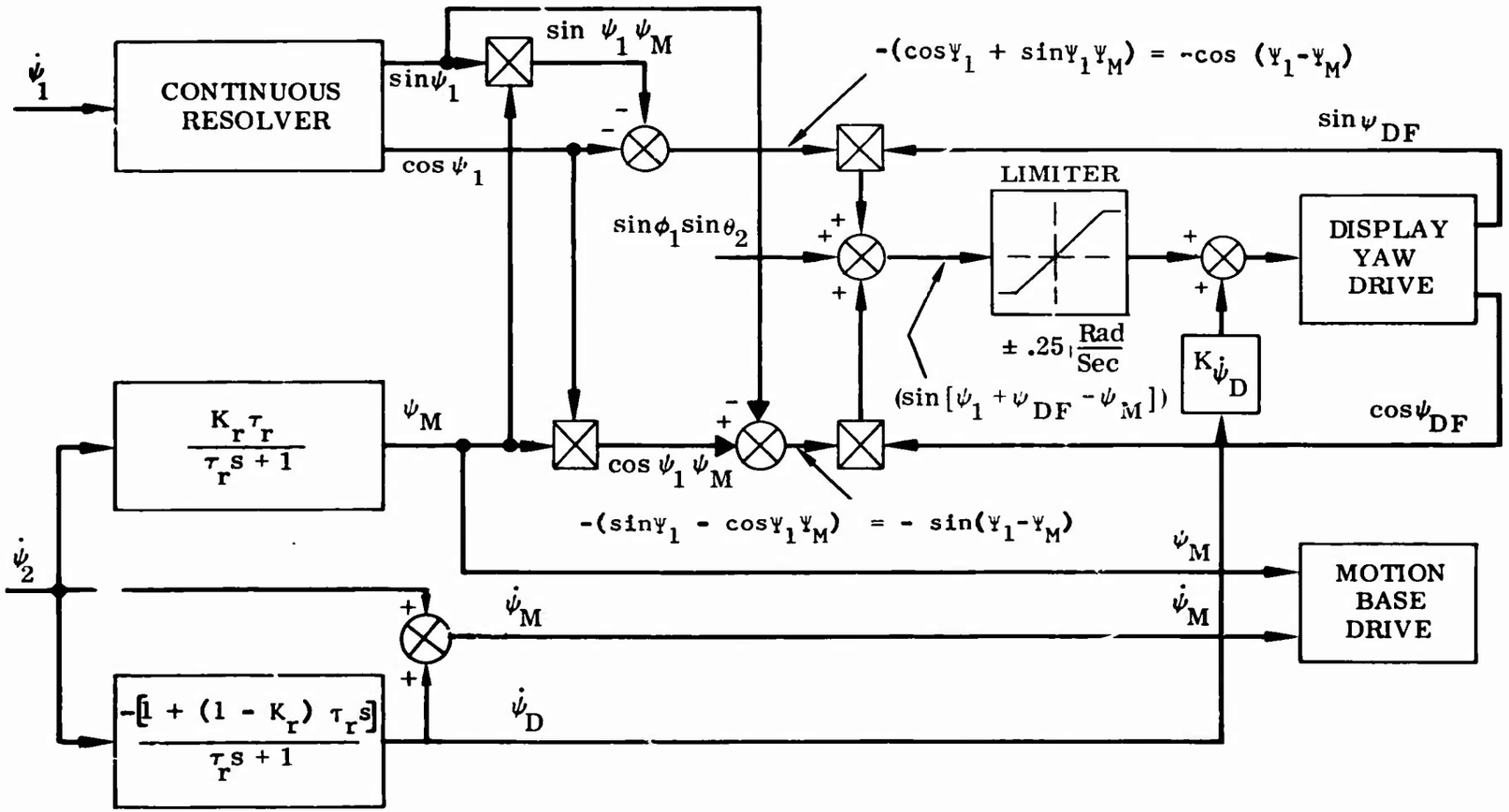

Figure 35. Mechanization B, Yaw Drive Details.

UNCLASSIFIED

Security Classification

DOCUMENT CONTROL DATA - R & D

(Security classification of title, body of abstract and indexing annotation must be entered when the overall report is classified)

1. ORIGINATING ACTIVITY (Corporate author)	2a. REPORT SECURITY CLASSIFICATION
Northrop Corporation Aircraft Division Hawthorne, California	Unclassified
	2b. GROUP

3. REPORT TITLE

APPLICATION OF THE NORTHROP ROTATIONAL SIMULATOR TO HELICOPTERS AND V/STOL AIRCRAFT (USER'S GUIDE)

4. DESCRIPTIVE NOTES (Type of report and inclusive dates)

Final Report

5. AUTHOR(S) (First name, middle initial, last name)

John B. Sinacori

6. REPORT DATE	7a. TOTAL NO. OF PAGES	7b. NO. OF REFS
May 1970	89	4

8a. CONTRACT OR GRANT NO.	9a. ORIGINATOR'S REPORT NUMBER(S)
DAAJ02-68-C-0019	USAAVLABS Technical Report 70-26
b. PROJECT NO. 1F162204A14233	
c.	9b. OTHER REPORT NO(S) (Any other numbers that may be assigned this report) NOR-70-6
d.	

10. DISTRIBUTION STATEMENT

This document is subject to special export controls, and each transmittal to foreign governments or foreign nationals may be made only with prior approval of U. S. Army Aviation Materiel Laboratories, Fort Eustis, Virginia 23604.

11. SUPPLEMENTARY NOTES	12. SPONSORING MILITARY ACTIVITY
	U.S. Army Aviation Materiel Laboratories Fort Eustis, Virginia

13. ABSTRACT

The purpose of this document is to suggest guidelines to be used in developing software interface computations so as to effectively integrate the pilot and mathematical vehicular representation to the Northrop rotational simulator.

A description of all key elements and their performance and operating characteristics is included. Past uses and projected future uses are also given. Some validation methods are described with suggestions for their use. Suggested interface mechanizations are given which provide effective visual and motion stimuli compatible with sensory characteristics. A rationale for the use of motion is included. A method is outlined which assists the user in assessing the probability of success in any desired simulation and preparation of an effective experimental design.

The document is considered incomplete because such information as is contained herein will be constantly updated and improved by subsequent users.

DD FORM 1 NOV 68 1473 REPLACES DD FORM 1473, 1 JAN 64, WHICH IS OBSOLETE FOR ARMY USE.

Unclassified

Security Classification

14. KEY WORDS	LINK A		LINK B		LINK C	
	ROLE	WT	ROLE	WT	ROLE	WT
Flight Simulation						
Simulator Validation						
V/STOL Simulation						
Helicopter Simulation						